Technische Universität München
Fakultät für Medizin

Comparing pre- and postoperative navigated transcranial magnetic stimulation mappings of cortical motor function in glioma patients

Neal Michael Conway

Vollständiger Abdruck der von der Fakultät für Medizin der Technischen Universität München zur Erlangung des akademischen Grades eines Doktors der Medizinischen Wissenschaft (Dr. med. sci.) genehmigten Dissertation.

Vorsitzender: Prof. Dr. Thomas Misgeld

Prüfer der Dissertation:

1. apl. Prof. Dr. Sandro M. Krieg
2. Priv.-Doz. Dr. Christian F. Sorg
3. Prof. Dr. Arthur Konnerth

Die Dissertation wurde am 06.09.2021 bei der Technischen Universität München eingereicht und durch die Fakultät für Medizin am 13.04.2022 angenommen.

Elements of this thesis have been published previously:

Conway, N., Wildschuetz, N., Moser, T., Bulubas, L., Sollmann, N., Tanigawa, N., Meyer, B., Krieg, S.M. (2017) “Cortical plasticity of motor-eloquent areas measured by navigated transcranial magnetic stimulation in patients with glioma,” *Journal of Neurosurgery*, 127(5), pp. 981–991. doi: 10.3171/2016.9.JNS161595.

ABBREVIATIONS

3D	three-dimensional
ADM	abductor digiti minimi
APB	abductor policis brevis
BCS	biceps brachii
CoG	center of gravity
DCS	direct cortical stimulation
DICOM	digital imaging and communications in medicine
EMG	electromyography
EOR	extent of resection
FCR	flexor carpi radialis
GBM	glioblastoma multiforme
GTR	gross total resection
HGG	high-grade glioma
HS	hotspot
IDH	isocitrate dehydrogenase
LGG	low-grade glioma
MEP	motor evoked potential
MFG	middle frontal gyrus
MR	magnetic resonance
MRI	magnetic resonance imaging
NBS	navigated brain stimulation
NIftI	Neuroimaging Informatics Technology Initiative
nTMS	navigated transcranial magnetic stimulation
PMd	dorsal premotor cortex
PMv	ventral premotor cortex
PoG	postcentral gyrus
POI	point(s) of interest (hotspots and centers of gravity)
PrG	precentral gyrus
rMT	resting motor threshold
rTMS	repetitive transcranial magnetic stimulation
SEM	standard error of the mean
SFG	superior frontal gyrus
SMA	supplementary motor area
TES	transcranial electric stimulation
TMS	transcranial magnetic stimulation
WHO	World Health Organization

TABLE OF CONTENTS

1. INTRODUCTION

1.1. Anatomy of the motor cortex

One of the most enduring topical descriptions of the human cortex was conceived by Brodmann in 1909. Based on the different cytoarchitectures he encountered at a microscopic level, he found that the cortex could be divided into 52 distinct areas, thereby creating a map of the cortex which is still commonly used for reference today (Brodmann, 1909; Jacobs, 2011). The hypothesis that the anatomically distinct Brodmann areas each hold specific functions seemed a logical and appealing one. It was therefore the subject of extensive research over the course of the 20th century, with varying results.

There are many models aimed at characterizing the organizational structure of the motor cortex based on their function rather than microanatomy, resulting in sometimes confusing or partially overlapping nomenclature. The motor cortex is most commonly divided into two major areas, the first of which is the primary motor cortex, usually taken to mean the precentral gyrus (PrG), with its corticospinal projections capable of inducing movement directly. Some sources use the term M1 as a synonym, or more specifically to describe the posterior part of the PrG, corresponding to Brodmann area 4. The remaining motor cortex is often called non-primary motor cortex, with the main criterion being that these areas cannot usually elicit movement directly, but rather induce it via cortico-cortical pathways, due to a perceived lack of corticospinal projections. It is often subdivided into the ventral and dorsal premotor corteces (PMv and PMd), as well as the supplementary motor area (SMA) (Foerster, 1936; Penfield and Boldrey, 1937; Chouinard and Paus, 2006).

Anatomically, the non-primary motor cortex is usually not quite as clearly defined as pertaining to a particular gyrus, but generally comprises areas frontal to the PrG, including the superior and middle frontal gyri (SFG and MFG). This clear differentiation, however, is subject to continuous alteration, not least due to evidence that direct corticospinal projections are, in fact, not exclusive to the PrG after all (Dum and Strick, 2002; Teitti *et al.*, 2008).

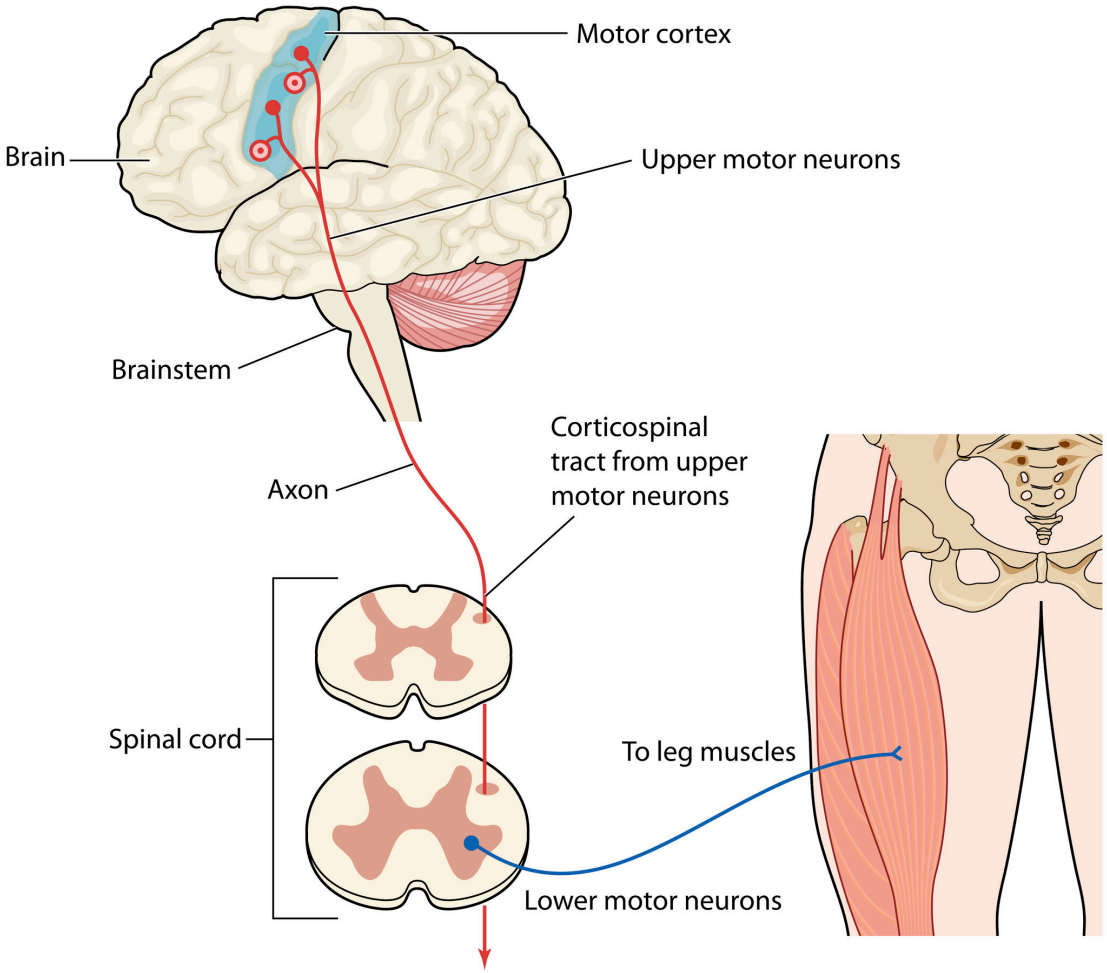

Figure 1 – pyramidal tracts
Schematic illustration of a corticospinal projection. Descending form the upper motor neurons of the motor cortex, these tracts form part of the white matter of the spinal cord, and, in most cases, synapse in the anterior horn cells contralateral to the side of the cortex they originated from. From the lower motor neurons in the anterior horn cells, transmission continues towards the nerve-muscle junctions (Peter Lamb © 123RF.com).

With regards to the function of non-primary motor areas, it is believed that they are chiefly responsible for planning and initiating complex movements, or, more broadly speaking, “can influence motor output” (Chouinard and Paus, 2006). The primary motor cortex, meanwhile, is the starting point of the pyramidal tracts. These are the descending neural pathways that control conscious movement of the contralateral half of the body, crossing over to that side at certain points along the spinal cord. The neurons whose axons form the start of these pyramidal tracts are arranged across the PrG in such a way that neurons controlling adjacent muscles can be found in nearby locations in the PrG. On a larger scale, this means that particular areas within the primary motor cortex represent the motor cortical equivalent of particular parts of the body, a concept called somatotopic organization (Penfield and Boldrey, 1937; Schieber, 2001).

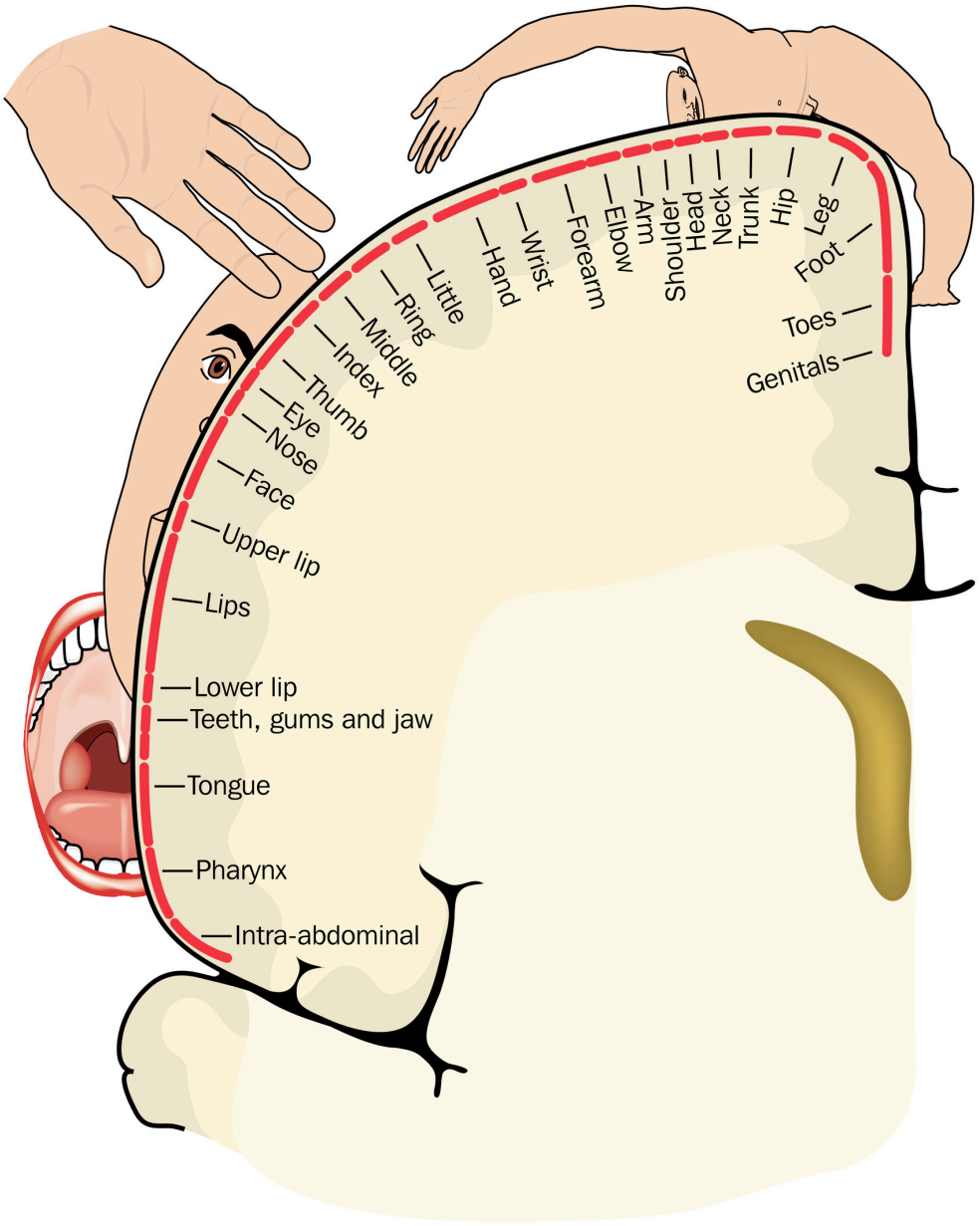

Figure 2 – the homunculus
Somatotopic distribution as illustrated by the human motor cortical homunculus. The image represents a schematic overview of the human motor cortex, specifically the PrG, in the coronal plane. Parts of the body are depicted next to the approximate areas of the motor cortex thought to be mainly responsible for the respective body parts' primary motor function (Peter Lamb © 123RF.com).

Although this overall concept has been confirmed multiple times, its initial interpretation, according to which each muscle would be exclusively controlled by a tightly defined area on the cortical surface, arranged in neat, somatotopic order relative to adjacent muscle representations, has largely been discarded. Rather, the current consensus holds that somatotopy applies to regions of the body, such as arm, leg and face, with interconnected and overlapping neural networks responsible for the triggering of movements within these body regions

(Sessle and Wiesendanger, 1982; Sanes and Donoghue, 2000; Massé-Alarie *et al.*, 2017). Indeed, it has been shown that even in the adult cortex, the physiological learning process correlates with a redistribution of primary motor function (Ungerleider, Doyon and Karni, 2002; Duffau, 2005). This fluid organizational structure suggests an inherent potential for adaptation to changing circumstances, as explored in the next section. The research presented in this thesis focuses on the motor cortical representation of the arm and hand muscles.

1.2. Cerebral plasticity and functional reorganization in glioma patients

Cerebral neuronal plasticity can be defined as "the capacity of the brain to change in response to experience, use, or environmental changes, and to injury of its own integrity" (Classen, 2013).. The term neuronal plasticity is sometimes subdivided into functional reorganization and structural plasticity, whereby the latter implies change through physical alterations to the neuronal structure, while the former refers to incidences in which parts of the brain take on functions they did not previously execute (Puderbaugh and Emmady, 2021). Subscribers to this terminology see plasticity as an umbrella term encompassing both phenomena, though others have argued in favor of a narrower definition: They take the view that in order for changes to be deemed "plastic" they must be both functional and structural in nature (Paillard, 1976; Will *et al.*, 2008; Berlucchi and Buchtel, 2009).

To avoid any confusion, this thesis uses the terms neuronal or cortical reorganization whenever an umbrella term for functional and structural changes to the nervous system or cortex is required, and specifies functional reorganization where we deem it appropriate.

The outlook on cortical reorganization has undergone considerable reevaluation in light of a series of findings indicating that the adult human cortex is capable of more change and adaptation than previously thought (Nii *et al.*, 1996; Sanes and Donoghue, 2000; Hayashi *et al.*, 2014). Mounting evidence shows the adult brain is capable of both functional reorganization and structural plasticity (Draganski *et al.*, 2004; Dayan and Cohen, 2011).

As referenced above, besides a range of physiological processes of learning, one major driving force for neuronal reorganization is structural damage to the brain itself. Hence, by definition, all fields of medicine focused on the diagnosis and subsequent treatment of damage to the central nervous system are concerned with neuronal reorganization. Not only must they study changes any given ailment may induce: Their treatments' success often relies on the brain's capacity to adapt to therapeutic interventions while suffering as little

functional deficit as possible (Duffau, Denvil and Capelle, 2002; Gil Robles *et al.*, 2008; Hayashi *et al.*, 2014).

Irrespective of possible mechanisms, it has become clear that the distribution – and re-distribution after injury – of cortical function is not limited to the confines of classic, rigid functional anatomy (Duffau, 2014a). Focusing on the motor cortex, researchers have found that corticospinal tracts can be found to originate beyond the PrG, in the SFG (Teitti *et al.*, 2008). While this does not necessarily mean that these pathways are regularly used to elicit movement, it does demonstrate the potential for other areas to take over the functions of the PrG should it incur harm in some way. Indeed, it has since been confirmed that primary motor function can be shifted to areas outside of the PrG, including the SMA (Ius *et al.*, 2011; Bulubas *et al.*, 2016; Moser *et al.*, 2017). Experiments and observations point towards a fluctuating, adaptive functional anatomy even in healthy individuals, where cortical representation of any particular function can change within days as a result of increased or decreased use (Hallett, 2000). As long as one relies chiefly upon empirical observations of cortical reorganization, it remains hard to predict how the brain will react to any given intervention, physical or otherwise.

A notable patient group for which an improved understanding of the brain's capacity for adaptation would have significant implications is that of glioma patients. Glioma is an umbrella term for tumors originating from astrocytes or oligodendrocytes, thus describing a group of primary neoplasms of the brain. They account for "81% of malignant brain and central nervous system […] tumors in the United States" (Ostrom *et al.*, 2017), and are graded by malignancy from World Health Organization (WHO) grades I to IV (Louis *et al.*, 2016). WHO grades I and II denote low-grade glioma (LGG), whereas WHO grades III and IV are known as high-grade glioma (HGG), including the particularly malignant glioblastoma multiforme (GBM)(Forst *et al.*, 2014). Previously a purely histological classification, the 2016 update to the WHO classification of glioma introduced molecular biomarkers, such as isocitrate dehydrogenase (IDH) mutation and 1p/19q codeletion, in order to better reflect the tumors' expected response to current and developing treatment strategies (Reifenberger *et al.*, 2016).

Though prognosis varies depending on tumor subtype, WHO grade and other considerations, symptoms, other than seizures, are largely determined by the tumor's location (DeAngelis, 2001). The logic here is that as the neoplasm infiltrates, presses on, or causes edema in certain areas of the central nervous system, the functions of these areas will be among the first to be adversely affected. This results in a diverse array of possible symptoms, notably including motor function impairment caused by a tumor affecting the primary motor cortex. Such impairments can have severe implications on patients' quality of life, and are therefore a major consideration when mapping out treatment strategies. This holds par-

ticularly true for treatments that may further damage the healthy brain tissue, thus potentially aggravating the impairment caused by the tumor itself. As glioma often develop in near proximity to eloquent regions, it is not uncommon for paresis to be caused by surgical treatment. Additionally, malignant tissue may itself still contain functioning elements, meaning that total resection is very likely to come at the price of paresis in such cases (Ojemann, Miller and Silbergeld, 1996; Schiffbauer *et al.*, 2001).

Though not all subtypes and grades of glioma are treated with the same strategy, one constant across all WHO grades is that the first therapeutic modality is surgery, which may or may not be accompanied by radiotherapy and/or chemotherapy (Reni *et al.*, 2017). In this context, it is worthwhile noting that the extent of resection (EOR) plays a major role in determining the outcome: while the EOR is a "significant prognostic factor" (Hollon *et al.*, 2015) in LGG, it has been shown that gross total resection (GTR) is essential in improving GBM patients' survival through surgery (Marko *et al.*, 2014; Hayhurst, 2017; Reni *et al.*, 2017). Though extensive surgery is beneficial from a purely oncological point of view (Suchorska *et al.*, 2016), there continues to be considerable debate over its effects on patients' quality of life after surgery. On one hand, it has been suggested that more complete resection reduces the likelihood of seizures (Rudà *et al.*, 2012). However, as referenced above, increasing the EOR also increases the risk of removing potentially eloquent brain, sometimes resulting in significant impairment. The lack of definitive, level I evidence regarding the trade-off between maximum resection and post-surgical impairment reinforced the concept of making these decisions on EOR on an individual, case-by-case basis (Schucht *et al.*, 2015; Hervey-Jumper and Berger, 2016; D'Amico *et al.*, 2017).

One central aspect in evaluating the cost-benefit ratio of surgery for a patient with glioma is, of course, the tumor's location relative to known "eloquent" regions of the cortex. Thanks to intraoperative monitoring via direct cortical stimulation (DCS), surgeons are able to go beyond the confines of received anatomic wisdom and tailor the EOR to the distribution of the patients' motor or speech function intraoperatively. This has helped to better preserve motor function, while increasing the EOR (Duffau *et al.*, 2005; Sanai and Berger, 2010). The obvious limitation here is the fact that this places intraoperative decisions at the center of therapeutic strategy, with two significant drawbacks: The patient cannot be consulted, and the decision-making process takes place in the setting of an ongoing surgical procedure, which may cause undue haste. In this situation, a preoperative, non-invasive and accurate mapping of cortical function can deliver clear benefits by improving surgical planning (Krieg *et al.*, 2012) and the patients' understanding of the planned and its possible implications, thereby improving informed consent (Jung *et al.*, 2019; Lavrador *et al.*, 2020). It has even been proposed that such preoperative mapping of cortical functions could be used to help with the timing of multi-stage surgery (Martino *et al.*, 2009; Duffau and Taillandier, 2015) as

witnessed in one case by Takahashi et al. (Takahashi *et al.*, 2012). This approach ultimately relies on functional reorganization of neural networks, a process that is as yet not understood to such a degree as to enable reliable predictions. In the next chapter of this thesis, we will focus on the methods established to help uncover and chart the often-changing networks of glioma patients' brains. It is integral that they continue to be refined to further the available knowledge on cortical reorganization and plasticity with a view to being able to reliably predict it, and thereby possibly integrate it as a reliable tool in a more complete therapeutic approach.

1.3. Navigated transcranial magnetic stimulation (nTMS)

The gold standard for localizing eloquent cortical regions has so far been intraoperative DCS (Forster *et al.*, 2011; Ottenhausen *et al.*, 2015). As implied by the name, DCS entails applying electrical stimuli directly to the surface of the cortex. When mapping cortical motor function, motor evoked potentials (MEP) – muscle contractions detected electromyographically as a result of prior stimulation – give immediate feedback on the role of neurons at the stimulated point (Penfield and Boldrey, 1937; Opitz *et al.*, 2014). This directness helped DCS become an established tool in neurosurgery. It provides surgeons with reliable information on where, in a physiological sense, they are operating, and helps them confirm or adapt preoperatively planned resection margins intraoperatively (Tamura *et al.*, 2015). However, in order to directly stimulate the human cortex, it is of course necessary to access it, meaning DCS requires craniotomy. DCS cannot, therefore, provide information for preoperative planning, denying surgeons the chance of taking reorganization or individual deviations from standard anatomy into account in advance. Hence the demand for a modality capable of mapping cortical functions prior to surgery (Krieg *et al.*, 2012).

One method addressing this shortcoming of DCS is transcranial electric stimulation (TES) – an approach essentially relying on higher voltage to compensate for the isolating layers of tissue of dura mater, skull, and scalp (Merton and Morton, 1980). Its potential however, has always been limited by the considerable amount of discomfort and pain that come with this increase in stimulation intensity (Klomjai, Katz and Lackmy-Vallée, 2015).

Hence, transcranial magnetic stimulation (TMS) has been brought to the fold, and is increasingly being used as a tool for preoperative planning thanks to the fact that it causes considerably less discomfort to the patient, and has been found to be safe (Tarapore *et al.*, 2016). Also, its measurements have been shown to concur with DCS to a high degree (Forster *et al.*, 2011). Amongst other benefits, it has allowed surgeons to reduce incision sizes and

operation times, measures that decrease the risk patients are exposed to during cranial surgery (Krieg *et al.*, 2012; Ottenhausen *et al.*, 2015).

1.3.1. Underlying principles of TMS

In contrast to DCS, and even TES, TMS does not require direct contact with the cortex to electrically stimulate it. It bridges the barrier of the scalp and the skull by inducing an electric field within the skull. To achieve this, a short-lasting, magnetic field of changing intensity – itself induced through the passing of an electric current through wire coils of various shapes – is applied to the area that one wishes to stimulate (Barker, Jalinous and Freeston, 1985; Hallett, 2000). The electric field induced on the cortical surface can cause the depolarization of neurons once a certain threshold is surpassed, leading to the temporary modulation of neuronal activity in the targeted cortical region (Hallett, 2000; Awiszus and Feistner, 2007; Ruohonen and Karhu, 2010; Horvath *et al.*, 2011).

1.3.2. Neuronavigation

In order to interpret the results of this modulation, it is of primary importance to determine which area was stimulated with the highest possible level of precision. This is where neuronavigation comes into play. It is now commonplace for TMS systems to include a monitor displaying a three-dimensional (3D) model of the patient's or test subject's cortical surface, based on previously recorded magnetic resonance imaging (MRI). Upon this model, the site of maximum stimulation that can be expected based on the stimulation coil's position is projected in real time (Ettinger *et al.*, 1998; Ruohonen and Ilmoniemi, 1999). With the help of this visualization, the researcher can not only selectively target specific regions more accurately. Stimulation points can also be recorded, allowing for more detailed analysis and the subsequent construction of "functional maps" of the cortex (Lioumis *et al.*, 2012). When neuronavigation is combined with TMS in this way, it is common to speak of "navigated TMS" (nTMS).

To correctly calculate the size and distribution of the electric field induced in the brain upon nTMS application, it is necessary to take various variables into account. The main factors relevant in this context are stimulation intensity, wire coil shape, and the angle at which the coil is positioned relative to the cortical surface at the time of stimulation (Brasil-Neto *et al.*, 1992; Ravazzani *et al.*, 1996; Ruohonen and Karhu, 2010).

A wide variety of coil shapes have been developed, with circular and the so-called figure 8 coil shapes being the most commonly used (Paulus, Peterchev and Ridding, 2013; Rossini *et*

al., 2015). As indicated in figure 3, the main advantage of the figure 8 coil over the simple circular coil is that the induced electrical field is more focused (Hallett, 2007). The point of maximum current induction, and therefore neuronal stimulation, is located directly beneath the center of the coil. In contrast, circular coils induce circular areas of maximum current induction, thereby stimulating a wider area of the cortex. Thus, in practice, the figure 8 coil allows researchers to better target points of their choice on the cortical surface (Groppa *et al.*, 2012).

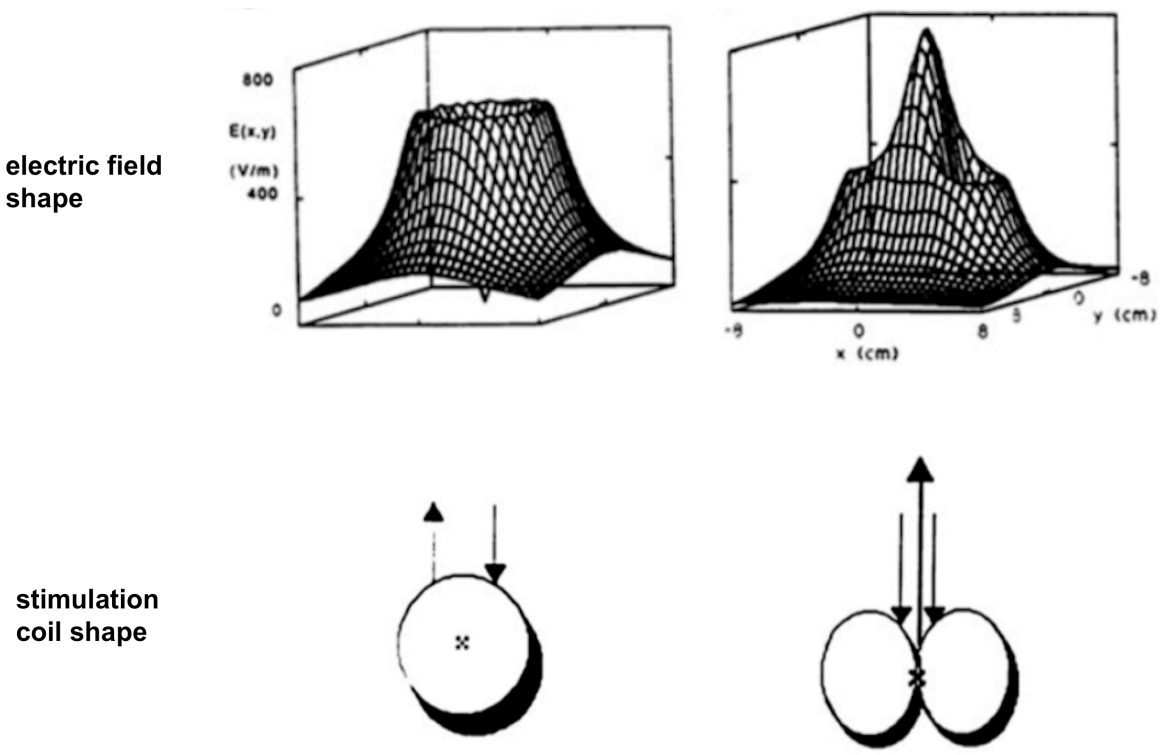

Figure 3 – electric field magnitude as a function of coil shape
The point of highest magnitude of the electric field generated by a TMS stimulation coil depends on how the coil is configured. This image illustrates the shape of an electric field generated by a circular coil (left half of image) compared to a figure 8 coil (right half of image). The origin of the coordinate system is defined as being 1cm below the center of the coil. While a circular coil generates an electric field with a ring-shaped maximum, figure 8 coils result in more tightly definable, singular points of maximum electric field magnitude (modified from Cohen and Panizza, 1990; Hallett, 2007).

To help an nTMS interface detect the position of the wire coil relative to the subject's head, stereotactic tracking equipment – already a staple of modern neurosurgery – is used. Based on this information, the data on the distribution of the electric field, and the MRI-based brain model mentioned above, modern nTMS systems then compute the expected site of stimula-

tion given the coil position and planned stimulation intensity at any given time (Ruohonen and Karhu, 2010).

For neuronavigation to work, the angle at which the stimulation coil is placed relative to the targeted gyrus must also be taken into account. This concept stems from the fact that "To effectively stimulate cortical neurons, the current flow in the tissue has to produce an outward directed trans-membrane current (ion-flow) in cortical axons" (Groppa *et al.*, 2012). It follows that the angle at which the wire coil is held during stimulation plays a major role in determining the stimulation intensity necessary to elicit a response, as well as which neurons are primarily stimulated (Sakai *et al.*, 1997; Opitz *et al.*, 2013). To accurately determine the site of neuron stimulation, it is mandatory that the area calculated to be the site of the induced electric field's maximum intensity is also the location of maximum neuron stimulation. The best way to achieve this, given the anatomical arrangement of cortical axons, is to ensure that the induced currents are at a right angle to the gyrus intended for stimulation, by placing the stimulation coil accordingly (Brasil-Neto *et al.*, 1992; Mills, Boniface and Schubert, 1992; Ruohonen and Karhu, 2010). It should be kept in mind that the electrical field induced in the brain is perpendicular to the magnetic field, which in turn is perpendicular to the orientation of the wire coil (Thielscher, Opitz and Windhoff, 2011; Klomjai, Katz and Lackmy-Vallée, 2015).

1.3.3. Applications

1.3.3.1. Motor function mapping

Thanks to the addition of neuronavigation, the mapping of cortical motor function with TMS has become a modality that is increasingly used in research as well as in clinical settings (Ottenhausen *et al.*, 2015). As with DCS, the order in which excitation takes place – from cortical motor neurons to muscle fibers – is no different from the physiological one. Put differently, the relationship between the stimulation point and subsequent muscle contraction is causal, which leaves far less room for (mis-) interpretation than, say, functional MRI or magnetoencephalography, both modalities that rely on mere correlation (Hess, Mills and Murray, 1987; Klomjai, Katz and Lackmy-Vallée, 2015; Ottenhausen *et al.*, 2015).

It has recently been shown that use of nTMS motor mapping before operating on lesions in motor eloquent cortex areas indeed allowed neurosurgical teams to reduce craniotomy size and even improved the overall outcome (Krieg, Sabih, *et al.*, 2014), demonstrating its merit as a preoperative planning tool.

1.3.3.2. Other applications

Though motor function mapping is the focus of this thesis, it is not the only area where nTMS has been found to have potential. Regarding other diagnostic applications, methods to produce maps portraying the distribution of cortical functions such as language and calculation have been developed and continue to evolve (Pascual-Leone, Gates and Dhuna, 1991; Picht *et al.*, 2013; Krieg, Sollmann, *et al.*, 2014; Rösler *et al.*, 2014; Giglhuber *et al.*, 2017; Ille *et al.*, 2018). In contrast to the single-pulse stimulation pattern used in TMS motor mapping, language and calculation mappings are based on repetitive TMS (rTMS). The repetitive stimulation is thought to have an inhibitory effect, or "virtual lesion" (Pascual-Leone, Bartres-Faz and Keenan, 1999), causing temporary speech arrest or calculation errors when applied to areas relevant to language or calculation, respectively (Hallett, 2007). While these methods for mapping higher cognitive functions have not yet reached the widespread use and acceptance in neurosurgery of nTMS motor mapping, they are increasingly being trialed as part of preoperative routine in a growing list of neurosurgical departments (Picht *et al.*, 2013; Krieg, Sollmann, *et al.*, 2014).

Beyond these diagnostic applications, the list of use-cases for TMS as a therapeutic tool continues to grow, and include a range of neuropsychiatric diseases from major depression, chronic pain, dystonia, Parkinson's disease, Alzheimer's disease, and stroke rehabilitation, to tinnitus, (Pascual-Leone *et al.*, 1994; Siebner *et al.*, 1999; Hallett, 2000; Fregni *et al.*, 2005; Kim *et al.*, 2006; Defrin *et al.*, 2007; Ahdab *et al.*, 2010; Naeser *et al.*, 2011; Janicak *et al.*, 2013; Perera *et al.*, 2016; Dong *et al.*, 2018). There has even been a recent pilot study exploring the possibility that rTMS could help with giving up cigarettes (Chang *et al.*, 2018). However, recent reviews noted that there is not yet enough consensus on the respective methodologies to appropriately pass judgment on the success of rTMS as a therapeutic modality (Bucur and Papagno, 2018; Iimori *et al.*, 2019).

1.3.4. TMS in research on motor cortical reorganization

The potential for therapeutic interventions, mostly centered around rTMS, is already a major example of how TMS can be of value to research on neural reorganization by inducing it. This thesis focuses on nTMS as a diagnostic tool for the detection of such reorganization, specifically of the motor cortex.

Early attempts to use TMS to demonstrate motor cortex reorganization were conducted in patients with lesions of peripheral nerves. It was demonstrated that the motor cortical representation of a limb will expand upon deafferentation – through amputation, paralysis, or even the mere application of a tourniquet – of that limb or region (Sanes, Suner and

Donoghue, 1990; Kew *et al.*, 1994; Rijntjes *et al.*, 1997; Seitz and Freund, 1997; Hallett, 2000). TMS-induced MEPs have been used to prove successful surgical connection of a chest wall nerve to a patient's paralyzed biceps, as well as the central nervous system's reaction: After a year, the primary motor neurons for the biceps were found to have been rerouted to the neurons responsible for the chest wall at spinal-chord-level, meaning that cortical hodotopy was restored by neuronal reorganization, thereby returning motor function to the biceps (Mano *et al.*, 1995; Hallett, 2000).

NTMS has also played a role in demonstrating the existence of functioning corticospinal tracts beyond the PrG in healthy subjects (Teitti *et al.*, 2008). Given their being necessary for the execution of fast movement, they are a prerequisite for any cortical area to perform primary motor function. Thus, the fact that they are present in parts of the cortex other than the PrG suggests it is theoretically possible for those parts to take on primary motor function. As for cases in which this potential is fulfilled, one medical field that has helped develop a better understanding of motor cortex reorganization with the help of nTMS is glioma surgery. As a by-product of the increased use of nTMS motor function mapping in neurosurgical patients, large amounts of data on cortical motor function distribution have become available. This has already spawned several research projects devoted to analyzing this data, including in our research group.

Analysis of 100 glioma patients' preoperative nTMS motor function mappings demonstrated that the location of cortical motor function was influenced by the position of the tumor (Bulubas *et al.*, 2016). This was then further substantiated by our study addressing the effects of the surgical removal of motor-positive nTMS mapping points anterior to the PrG. Beyond the fact itself that relevant primary motor function was found outside the PrG, the subsequent onset of permanent paresis upon resection of the sites in question verified their authenticity and relevance (Moser *et al.*, 2017).

One disadvantage that these research projects had in common was the lack of functional motor mapping at any post-surgical stage. The patients involved had, of course, not been subjected to nTMS motor mapping prior to the onset of their glioma. Functional reorganization was, in a sense, inferred, but not directly witnessed by comparing two or more motor function mappings by the same modality. Forster et al. intended to pave the way towards correcting this shortcoming, by demonstrating the repeatability of nTMS motor function mappings before and after surgery (Forster *et al.*, 2012). If functional reorganization were to continue in spite of, or because of, surgical intervention, repeat mappings after surgery could be used to visualize and monitor the resulting changes. With a sample size of only five patients, the results need to be interpreted with caution. However, given how little the patients' motor maps were found to differ before and after surgery, the study did serve as an indication that, barring cortical reorganization, nTMS can deliver consistent mappings

despite intermittent brain surgery. In contrast to the stability of motor cortical representation demonstrated by 4 out of 5 patients in that study, one presented a significant motor function shift in an anterior direction (Forster *et al.*, 2012). Similarly, Takahashi et al. reported on the case of an LGG patient whose motor map had shifted from the PrG to the postcentral gyrus (PoG) (Takahashi *et al.*, 2012).

These two studies suggest that nTMS should be suitable for the detection of functional reorganization occurring in glioma patients upon surgical tumor removal. They call for similar studies on a larger scale. Given that nTMS motor function mappings are conducted before any surgery involving the motor cortex at our center, we were well placed to conduct such a study. As delaying surgery for scientific benefit alone was ethically out of the question, we decided to arrange postoperative mappings in the hope of tracing cortical changes in this way.

1.4. Goals of this study

As detailed above, nTMS is used to detect how a person's cortical functions are distributed, which, in the case of glioma patients, allows for an individually tailored surgical approach. One preoperative function mapping by itself, however, does not conclusively determine whether the deviations from standard functional anatomy that may be observed are a mere anatomical variant, or adaptive changes caused by the patient's intracranial tumor. The objective of the study that lay the foundations for this thesis was to further explore the capacity of pre- and post-surgical nTMS to detect and measure shifts of the motor cortical representation of hand and arm muscles on the cortical surface as an indication of lesion-induced functional reorganization in glioma patients. A reliable method to track such changes could significantly enhance treatment strategies.

The core hypotheses tested in this project were therefore the following:

- Glioma can cause changes to the distribution of cortical motor function
- These changes can be traced with the help of nTMS motor function mapping

Furthermore, we aimed to obtain preliminary data on the frequency of such functional reorganization, and patterns regarding the direction or timing of redistribution. The group examined for these purposes consisted of patients undergoing glioma surgery.

2. MATERIAL AND METHODS

2.1. Ethical Standards

The study was approved by the Technical University of Munich's ethics committee, and deemed to be in accordance with the declaration of Helsinki (registration numbers 2793/10, 5497/12). All patients were informed on the study's methods, risks and objectives before each nTMS motor mapping, and gave their written consent (Conway *et al.*, 2017).

2.2. Study Design

Our study was designed as a prospective, non-randomized study. To be able to examine the effects glioma in the region of the PrG may have on the cortical localization of motor function, patients with such gliomas each underwent two nTMS motor mappings: one mapping before tumor resection, and a second 3-42 months after that surgery. The two resulting maps of each patient's motor function were then compared in order to detect any positional shift. To test for factors that may have influenced the direction and/or extent of such shifts, the data were split into subgroups.

2.3. Patient Cohort

22 glioma patients, 9 female and 13 male, were included in our study. Their ages ranged from 26 to 78 years, with a mean age of 49.6 years. For a patient to be considered for inclusion, their glioma needed to involve the PrG, or be located in close proximity to it. All patients underwent glioma resection surgery. Patients under 18 years of age were excluded from the study. Any patients fulfilling general exclusion criteria for either MRI or cranial TMS were also excluded. Such criteria include pacemakers, cochlear implants, and deep brain stimulation devices.

Subgroups were formed based on tumor location. We differentiated between group A, containing all patients whose tumors were situated anterior to the PrG, and group P, with patients whose tumor was considered to be located posterior to the PrG.

Table 1 – patient cohort
An overview over the patient cohort included in the present study. A patient's ID refers to their unique identifying number after anonymization. Groups "A" and "P" were formed based on the tumor location, with A including all patients with tumors anterior to the PrG, as opposed to P with the patients suffering from tumors posterior to the PrG, Further abbreviations not previously explained: "R": right hemisphere; "L": left hemisphere; "perm.": permanent; "trans.": transient; "comp.": complete; "sub.": subtotal, "med.": median (includes data from Conway *et al.*, 2017).

ID	age	gender	WHO grade of tumor	tumor side	group	time interval between maps (months)	tumor growth between maps 1 and 2	motor deficit at map 1	motor deficit at map 2	surgery -related motor deficit	EOR
1	41	m	2	R	A	9.5	no	no	yes	perm.	comp.
2	52	m	2	L	A	31.0	yes	no	no	none	sub.
3	60	f	4	L	A	11.5	yes	yes	yes	none	sub.
4	60	m	4	R	A	18.7	yes	no	no	none	comp.
5	31	m	1	L	A	21.9	no	no	no	none	comp.
6	46	f	3	L	A	16.0	yes	no	no	none	sub.
7	69	m	4	R	A	3.6	yes	no	no	none	comp.
8	36	m	3	R	A	10.5	yes	no	no	none	comp.
9	26	f	2	L	A	3.0	no	no	no	none	comp.
10	38	f	3	L	A	3.6	no	no	no	none	sub.
11	73	f	3	R	A	6.0	yes	yes	yes	perm.	sub.
12	40	f	2	R	A	5.1	no	no	no	none	comp.
13	53	m	3	R	P	41.2	yes	yes	yes	none	comp.
14	49	m	4	L	P	29.7	yes	no	no	none	comp.
15	40	m	4	R	P	6.0	yes	yes	yes	none	comp.
16	36	m	2	L	P	15.7	yes	no	no	trans.	comp.
17	27	m	4	L	P	6.0	yes	no	no	none	comp.
18	58	m	4	R	P	7.2	yes	yes	yes	none	comp.
19	48	f	3	R	P	5.2	no	no	no	trans.	sub.
20	73	f	4	R	P	6.8	yes	no	no	none	comp.
21	78	f	4	L	P	5.9	yes	no	yes	none	sub.
22	58	m	4	L	P	3.0	yes	no	yes	none	sub.
mean	49.6		3.1			12.1					
SEM	3.2		0.2			2.2					
min	26		1			3.0					
max	78		4			41.2					
med.	48.5		3			7.0					
								p=0.5098			

2.4. MRI

Each patient received cranial MRI scans before each mapping. A 3-Tesla scanner with an 8-channel phased array head coil (Achieva 3T, Philips Medical Systems B.V) was used, and sequences included 3D gradient echo sequences and T2-weighted FLAIR (Conway *et al.*,

2017). Images of the former were saved in the “digital imaging and communications in medicine” (DICOM) format and then used for navigation during nTMS motor mapping.

2.5. nTMS Motor Mapping

2.5.1. System components

For nTMS motor mapping, we used the Nexstim eXimia NBS (Navigated Brain Stimulation) System (eXimia 4.3, Nexstim Oy). It features a figure 8 stimulation coil, which can be triggered via a foot pedal. To measure muscle response to stimulation, the system also features electromyography (EMG). Its six pairs of EMG electrodes (Ag/AgCl electrode, Neuroline 720, Ambu), are attached to muscles considered as corresponding to particular regions of the motor cortex, while a grounding electrode should be placed on the patient’s elbow or the ulnar styloid process.

To allow for localization of the patient’s head relative to the stimulation coil, the system features a 3D infrared tracking system (Polaris Spectra), coupled with corresponding spherical motion sensor tracking orbs attached to both the stimulation coil and a specially designed frame of glasses, as shown in figure 6 (the headband seen in figure 4 was not used in this study, to minimize the risk of dislocation). All components are connected to, and controlled through, the system’s computer interface.

2.5.2. Mapping protocol

2.5.2.1. Registration

In order to make sure that intracranial stimulation sites are computed correctly, the aforementioned tracking system requires prior calibration, by means of what is termed “registration” within our NBS system’s software. This entails first selecting superficial anatomical landmarks within the patient’s cranial MRI images, and then touching those landmarks with a “digitizing pen” which essentially consists of tracking orbs connected to a pointer in the shape of the letter “Y”. The software then cross-references the obtained positional data with an MRI-based 3D reconstruction of the patient’s brain. This means that, after finer calibration by means of tracing 9 further points on the patient’s scalp with the digitizing pen, the exact position of the patient’s head relative to that of the tracking glasses, and thereby, more importantly, relative to the stimulation coil, is detected by the tracking system with a margin of error of approximately 6.7mm (Corneal, Butler and Wolf, 2005; Ruohonen and Karhu, 2010; McGregor *et al.*, 2012; Sollmann *et al.*, 2013; Weiss *et al.*, 2013; Forster *et al.*, 2014).

Figure 4 – registration
As described in the text, registration was conducted with the help of a Y-shaped “digitizing pen”. The spherical orbs attached to both the pen and the patient’s head are registered by the infrared tracking sensor (Polaris Spectra), seen in the top left corner of this image. The headband on display here was not used in this study in favor of a more rigid construction, shown in figure 6.

With the resulting data, the NBS software then calculates which parts of the cortical surface can be expected to be reached by a stimulation pulse based on the stimulation coil’s real time position. It continuously feeds a visualization of these calculations to the user interface, allowing the investigator to deliberately target specific cortical surface structures during the mapping procedure.

2.5.2.2. EMG

Before stimulating the cortex with nTMS, the EMG electrodes need to be placed over muscles expected to produce MEPs upon stimulation of the contralateral hemisphere. As is common practice (Mills, Boniface and Schubert, 1992; Conforto *et al.*, 2004), we applied one electrode to the skin covering each targeted muscle belly, and a second one to the respective corresponding tendon.

To map the motor function of the upper extremity, we originally selected four muscles: the abductor policis brevis (APB), abductor digiti minimi (ADM), flexor carpi radialis (FCR), and biceps brachii (BCS) muscles. However, a large number of EMG channels also increases the likelihood and frequency of artifacts appearing in those channels. Such artifacts, when registered immediately, can disrupt the mapping process. Often caused by voluntary or subconscious muscle tension, they can lead to false positive readings upon stimulation. When noticed after the mapping is complete, it can be hard to tell such occurrences apart from actual MEPs. Seeing as the BCS muscle was often particularly susceptible to this issue, registration of its EMG was abandoned in a number of patients' mappings. We therefore did not use data on the BCS muscle in further analysis.

Concerning the lower extremity, we monitored the electrical activity of the tibialis anterior and gastrocnemius muscles. However, as the leg muscles' cortical representation is arranged along the medial longitudinal fissure, it is hard to reliably stimulate through nTMS, often requiring high stimulation intensities (Groppa *et al.*, 2012). In cases where high intensities were required, but mapping of the cortical representation of the leg was not necessary for surgical planning, motor mapping of that region was sometimes kept to a minimum or not conducted. To avoid drawing false conclusions from the resulting incomplete data, we decided against further analysis of motor mappings of leg muscles for the purposes of this study.

2.5.2.3. Resting Motor Threshold (rMT)

In line with common practice, we determined the rMT – the minimum necessary to cause an MEP – before conducting the nTMS mapping itself (Conforto *et al.*, 2004; Groppa *et al.*, 2012; Rossini *et al.*, 2015). To this end, each patient's PrG was stimulated with an intensity of 30% of the maximum available stimulation output. In the rare cases that this was not enough to provoke a motor response in the patient's contralateral arm despite several attempts at locating a suitable stimulation site, the stimulation intensity was increased very gradually, always making sure that the patient felt no discomfort. After stimulating a range of points along the PrG, the point at which the strongest MEP was elicited was earmarked for further confirmation. This confirmation was achieved by repeatedly stimulating said point to check for reproducibility. If repeat stimulation at that point caused an MEP of over 50μV three times out of five, the angulation of the coil was optimized for maximum MEP response, and

the most successful angle was then used during the rMT determination sequence, which is conducted semi-automatically with the help of the NBS software. As long as the investigator holds the stimulation coil in the correct position, it applies a series of stimuli of varying intensity, in search of the minimum stimulation intensity necessary to induce an MEP of over 50μV. This intensity is the rMT, and is calculated as a percentage of the coil's maximum output.

2.5.2.4. Stimulation

Having determined the rMT, we proceeded to apply that level of stimulation intensity, multiplied by a factor of 1.1, to map the motor function of the hand and arm. Starting at the site – usually at or around the part of the PrG often described as the "hand knob" (Yousry *et al.*, 1997) – previously used to determine the rMT, we moved the stimulation coil slightly before each new stimulation, thereby targeting an adjacent point on the cortex. Given immediate feedback through the interface as to whether the latest stimulation had indeed induced an MEP of over 50μV, we continued applying stimuli, ultimately creating a circular pattern centered around the area inducing the largest MEPs.

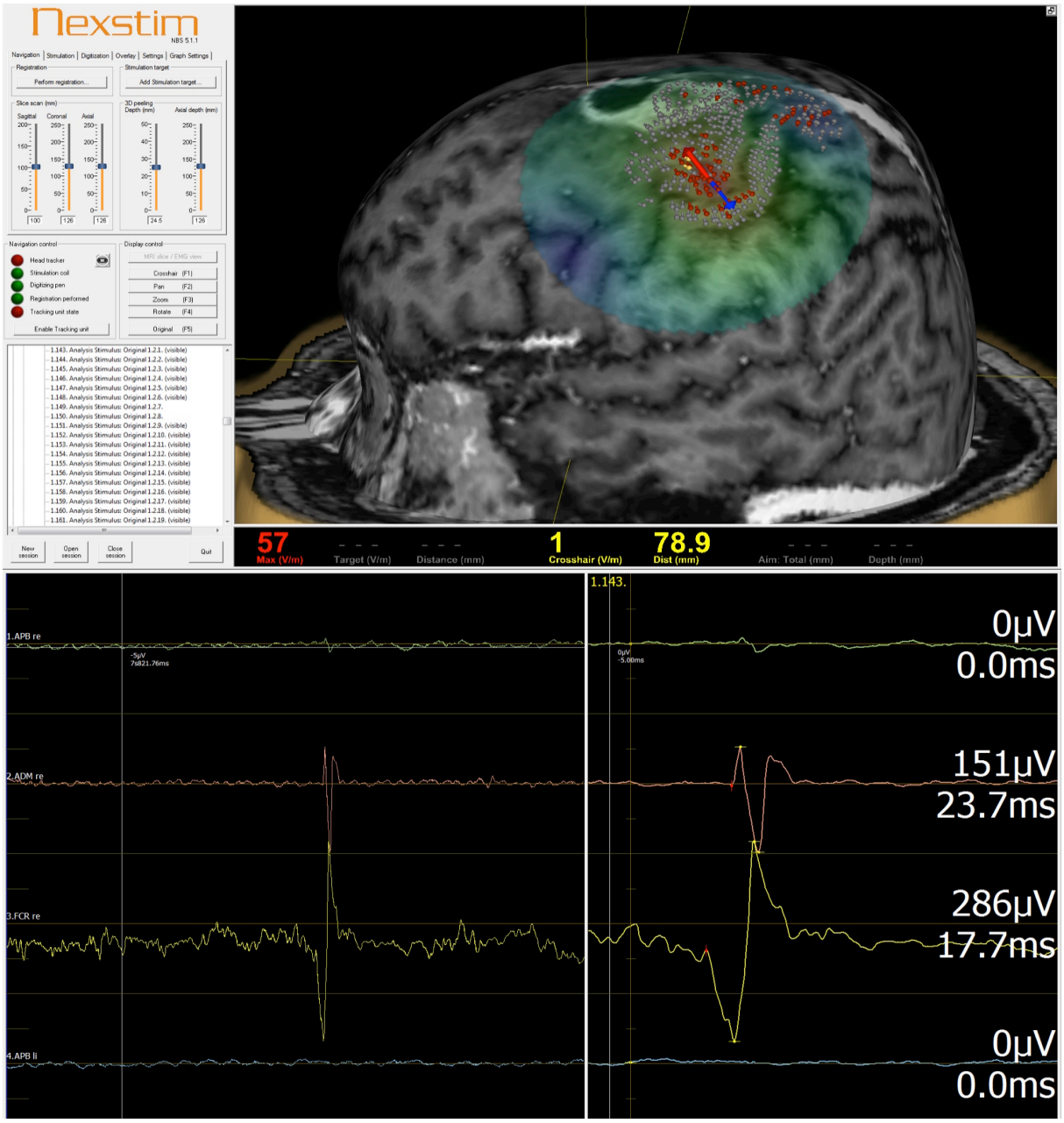

Figure 5 – interface screen shot
Screen shots of the NBS mapping software interface. The interface consists of two screens. Here, they are arranged vertically. Image settings, including depth and orientation, can be set using the grey panel on the left of the first screen. Also featured on the panel are status indicators for the tracking system, and a list of the points stimulated so far. Adjacent to it, the patient's 3D MRI is displayed, based on the aforementioned depth and orientation settings. The double arrow at the center of the translucent circle indicates the point of maximum stimulation on the cortical surface, as calculated by the system based on the relative positions of skull and stimulation coil. Not the perpendicular orientation of stimulation and gyrus. Red and yellow markers indicate stimuli that induced a motor response of over 50μV, grey markers represent those that did not. In this case, 4 muscles were mapped, resulting in 4 EMG recordings: APB, ADM, FCR, and the ipsilateral APB. The second screen shows patient's EMG readings around the time of the last stimulus, indicated by a white vertical line. The x axis displays time in ms, and the y axis shows the EMG response in μV. The same moment is shown twice, the difference being the unit spacing on the x axis. This allows for a more detailed view of the stimulus curve on the right side of the EMG screen, with tighter spacing of units on the x axis.

As discussed in the introduction, the stimulation coil should always be aligned in such a way that the vector of the resulting electrical field, as computed in real time by the NBS software, is perpendicular to the gyrus one intends to stimulate (Mills, Boniface and Schubert, 1992; Sakai *et al.*, 1997; Ruohonen and Karhu, 2010; Klomjai, Katz and Lackmy-Vallée, 2015). See figure 5 for an example of this.

For cortical motor function mapping of the lower extremity, we used a stimulation intensity of 1.3*rMT. In some patients, this was not enough to elicit an MEP of over 50μV, so that – if it was tolerable for the patient – we carefully increased the stimulation intensity to levels that did induce measureable MEPs.

For various reasons (logistics, other preoperative appointments taking up the patients' time, limited patient compliance) we could not carry out mappings of the contralateral hemisphere or the lower extremities in a significant number of patients. Mappings of the contralateral hemisphere or the lower extremities were therefore not taken into account for further analysis due to the scarcity of data.

Figure 6 – mapping setup
The stimulation coil is held to the subject's head, and positioned so that the direction of the electric field is perpendicular to the cortical surface. The NBS interface gives real-time feedback on whether this is the case. If so, the researcher can apply stimuli through a foot pedal (not pictured). In this image, the subject has been fitted with two electrodes to measure action potentials from the contralateral APB muscle, as well as one grounding electrode on the ipsilateral ulnar styloid process. The stimulation locations, as well as the corresponding EMG readings, are displayed and stored by the software.

2.6. Data Analysis

2.6.1. Pre-analysis

After each mapping, each piece of EMG reading that had been recognized by the NBS software as an MEP was checked for inconsistencies, such as particularly long latencies or high amplitudes, by an experienced investigator. The goal of this was to remove obvious artifacts due to any conscious or subconscious muscle contraction, or manipulation of the electrodes or wiring.

In 6 patients' cases, it became apparent during or shortly after the mappings that we were unable to acquire sufficiently clear EMG readings from individual muscles in one or both of the mappings. This caused us to discard the data on the muscles concerned from those patients' respective other mappings, thus using only data on muscles we had conducted two cortical motor function mappings of.

2.6.2. Hotspot (HS)

In the context of an nTMS motor function mapping, the HS for a particular muscle is the point on the cortical surface which, upon stimulation, leads to the strongest MEP in that muscle registered over the course of the mapping.

Before selecting the HSs for each muscle, a second examination of the raw mapping data was conducted by an experienced investigator, to minimize the likelihood of an artifact being selected as the HS. Criteria for the verification of MEPs included latency, graph shape, and coil angulation.

2.6.3. Map center of gravity (CoG)

As a second means of gauging the position of the cortical representation of a muscle, we chose the motor maps' CoGs for our analysis. Unlike the literal CoG of any physical object, a motor map's CoG takes into account not the distribution of physical weight, but rather the distribution – across the motor cortex – of the capacity to generate high-amplitude MEPs. This makes the map CoG less susceptible to artifacts, and more representative of the distribution of a muscle's cortical representation.

2.6.3.1. Theory

Our approach to computing the CoG was similar to a method by Koenraadt et al. (Koenraadt *et al.*, 2011). As detailed in our paper, "the CoG of x is a weighted mean of x, where the

weight (notated as w) is the relative EFmax [maximum electric field] amplitude" (Conway *et al.*, 2017). The motor map CoG for each analyzed muscle of each patient was computed in Microsoft Excel, on the basis of coordinates exported from the NBS software, using the following formulae:

$$CoG_x = \frac{\sum_{i=1}^{n}\left(EFmax_i \times x_i\right)}{\sum_{i=1}^{n} EFmax_i} \qquad CoG_y = \frac{\sum_{i=1}^{n}\left(EFmax_i \times y_i\right)}{\sum_{i=1}^{n} EFmax_i} \qquad CoG_z = \frac{\sum_{i=1}^{n}\left(EFmax_i \times z_i\right)}{\sum_{i=1}^{n} EFmax_i}$$

2.6.3.2. Practical considerations in this study

As a further safeguard against potential artifacts disrupting the data in the ways discussed above, a latency filter was included in the calculation. Thereby, for an MEP's stimulation coordinates to be used in CoG calculation for any particular motor mapping, the latency between stimulation and ensuing muscle contraction as registered through the EMG could not differ more than 5ms from the median of all such latencies registered for the muscle concerned during that mapping. The resulting CoG coordinates were then used to establish which mapping points came closest to the calculated points, so that these could later be used for visualization and positional comparison.

2.6.4. Normalization and cost-function masking

Each patient's HSs and map CoGs for the APB, ADM and FCR muscles were selected within the NBS software, and exported to the DICOM format as an overlay for display over the patient's magnetic resonance (MR) images, which were also exported to DICOM. These DICOM images and overlays then needed to be transferred to the Neuroimaging Informatics Technology Initiative (NIfTI) format, a conversion we completed using the dcm2nii software tool (McCausland Center for Brain Imaging, University of South Carolina).

The presence of a tumor, or the removal of both healthy and malignant intracranial tissue can cause the surrounding brain tissue to change its position within the cranium. This, in turn, clearly influences any attempt at measuring positional changes of elements within that brain tissue.

To counter these effects, the decision was taken to normalize the MR images and overlays, using the cost-function masking approach propagated and described by Brett et al. (Brett *et*

al., 2001). The decision was based on observations made by other research groups that this remained the method of choice for normalization of images depicting focally lesioned brains (Andersen, Rapcsak and Beeson, 2010).

The normalization of a patient's MR images and HS and CoG overlays, all in the NIfTI format, was computed in SPM12 (Functional Imaging Laboratory, Wellcome Trust Center for Neuroimaging, Institute of Neurology, UCL, London, UK) on the basis of a standard brain image with a resolution of 2mm named "single subj_T1.nii", which was provided as part of the software package.

2.6.5. Change Evaluation

In order to gauge the extent of potential positional changes of the motor cortical representation of the hand and arm that may have taken place between a patient's two mappings, we employed two distinct methods. Besides measuring the difference between the positions of various HSs and CoGs at the two time-points, we chose to complement this approach with a visual analysis as a means of double-checking the results obtained through Euclidian measurement.

2.6.5.1. Coordinates-based measurement

Normalizing the native MR images as well as the overlays displaying the HSs and CoGs (hereafter grouped under the umbrella term points of interest or "POIs") registered and computed as detailed above, brought with it the benefit of being able to compare the positions of any two POIs within the image series' 3D coordinates. This also applied to two points that were not necessarily registered in the same mapping, allowing for direct comparison of the potentially differing positions of HSs and CoGs between two mappings of the same cortex.

We therefore observed the coordinates of each POI using mriCron, and transposed those coordinates to the following coordinate system for use in our further analysis: the x axis represents the mediolateral axis, originating from the midline; the y axis represents the posteroanterior axis, and originates at the posterior-most point of the normalized image; while the z axis represents the inferior-superior axis.

Within this coordinate system, we proceeded to calculate the distances between the first and second measurements of each POI on the x and y axes. The inferior-superior z axis was not taken into consideration for further analysis, as the aim of our research was to find changes of POI positions along the cortical surface, for which the x-y-plain was accepted as a viable approximation.

The coordinate system used opened up two ways of comparing the positions of POIs across mappings. The first was to simply measure the distance between POIs from the first and second mappings, and express this distance as a positive value, i.e. the magnitude of the resulting vectors and the absolute values of the vectors' respective components. This approach enabled us to compare the extent of POI shifts observed in any given patient to the extent of such shifts observed in another. However, it was limited to describing how much positional change had taken place on which axis. It did not contain information regarding the respective directions of these changes on the axes concerned.

The second means of measuring positional changes of POIs with the aforementioned coordinate system took direction into account, by describing each positional change between mappings as an increase or decrease of x and y values. Rather than describing the vector's magnitude, this approach enabled us to describe in what direction shifts had been observed along each axis. Positive values meant that POIs were found to be further lateral on the x axis or anterior on the y axis at the second mapping than they had been at the first. Negative values, accordingly, represented shifts towards positions situated further medial on the x axis, or posterior on the y axis.

2.6.5.2. Visual comparison

Besides the coordinates-based measurement of positional shifts of POIs, we conducted a cursory further assessment of such changes through visual analysis. To this end, we compared the unedited 3D visualizations of each patient's two mappings. An example of how the images were used for this analysis can be seen in figure 11, to be found in the results section. The main thinking behind this approach was that, although the differences observed were not objectively quantifiable, the images had not yet been subjected to normalization, ensuring that any potentially counter-productive distortion that may have been caused by that normalization does not play a role in this mode of analysis.

This visual analysis was focused on excluding or uncovering any gross miscalculations with regards to determining the direction and approximate extent of any observed shifts. It also had the goal of confirming which gyrus or area POIs were calculated to have shifted towards, particularly in relation to the PrG and each patient's tumor location subgroup. Furthermore, we checked whether the shifts observed appeared to be associated with the occurrence of edema or particularly extensive surgical trauma.

2.7. Statistical Analysis

Graph Pad Prism version 6.04 was used for all statistical analysis in this study. Results are presented as the respective mean ± standard error of the mean (SEM). In order for a result to be considered statistically significant, p needed to be below 0.05.

2.7.1. Extent of shifts

2.7.1.1. Extent of shift by axis

Wilcoxon matched-pairs signed-rank tests were used to analyze the extent to which POIs were found to have shifted along the posteroanterior y-axis compared to the extent of such shifts along the mediolateral x-axis.

2.7.1.2. Extent of shifts in relation to size of time interval and tumor grade

A further aim of this study was to uncover any potential relationship, linear or otherwise, between the time between a patient's two mappings (Δt), and the extent of POI shift along the cortical surface adjudged to have taken place in that time. To this end, linear regression was performed.

As a means of shedding light on whether the grade of a patient's tumor influenced the relationship between Δt and the extent of POI shift, linear regression was also computed separately for patients with low-grade and high-grade tumors. For these purposes, WHO grades 1 and 2 were considered low-grade, with WHO grades 3 and 4 deemed high-grade tumors.

2.7.2. Subgroup-based analysis of shift direction

Changes of POI position as measured on the posteroanterior and mediolateral axes, respectively, were then analyzed separately for each group formed based on tumor position. The direction of the observed shifts was taken into account for these analyses, with anterior and lateral shifts denoted as positive shifts, while posterior and medial shifts were denoted as negative shifts. To test any differences between the groups for significance, Mann-Whitney-U-tests were employed.

2.7.3. 10-mm cut-off count

To objectively quantify the number of shifts, notably to draw conclusions on the frequency of functional reorganization in glioma patients, it was necessary to differentiate between definite

shifts of primary function and possible artifacts. Various inaccuracies are inherent to the methods employed for collecting the data this study is based on. These include the margin of error of the neuronavigational component of the NBS system, calculated to by Ruohonen and Karhu to measure an approximate 5.7 mm (2010). Further sources of inaccuracy are the fine but nevertheless potentially distorting resolutions of both the native MR images and those provided by the SPM software to form the basis of normalization, at 1mm and 2mm respectively.

To ensure that the effects these issues could have on the analysis could be taken into account, a 10-mm cut-off was applied to the shift vectors along the cortical surface. Any shift above this margin was deemed a definite shift, with shifts below this threshold seen as possible artifacts for the purpose of counting the number of patients presenting with functional reorganization. Statistical analysis including supra-threshold shifts only could not be computed for mathematical reasons. The 10-mm cut-off was applied to both tumor location groups to evaluate the distribution of supra-threshold shifts across groups.

2.7.4. rMT analysis

To help monitor the degree to which the patients' rMTs changed between mappings, we calculated the coefficient of variance for each patient's set of rMT values.

To evaluate potential changes of rMT levels between mappings, a paired t-test was conducted comparing rMTs from preoperative mappings to those measured at postoperative mappings.

3. RESULTS

3.1. Extent of shifts

3.1.1. Overall extent of shifts

Upon comparison of the absolute values of POI shifts observed on the x and y axes, it became apparent that the extent to which these shifts occurred was significantly greater on the y axis than on the x axis. The average value of HS shifts was 5.1mm ± 0.9mm on the x axis, and 10.7mm ± 1.6mm on the y axis, while CoGs were found to have moved by an average 4.6mm ± 0.8mm on the x axis, and 8.7mm ± 1.5mm on the y axis. All shift vector values are displayed in table 2 (Conway *et al.*, 2017).

To allow for a better overview, overall POI shift value averages were calculated, taking both HS and CoG shifts into account: hence, overall, POIs were found to have shifted by 4.7mm ± 0.8mm on the x axis, and 9.7mm ± 1.5mm on the y axis. Shifts as measured for HSs and CoGs individually can be found in table 2.

Statistical analysis concluded that the extent to which HSs, CoGs, and POIs in general, were found to differ in location between mappings was significantly greater on the posteroanterior y axis than it was on the mediolateral x axis ($p=0.0011$ for HS; $p=0.0075$ for CoG; $p=0.0008$ for POI overall) (Conway *et al.*, 2017). Bar charts showing the average extent of shifts by axis can be found in figure 7.

Table 2 – overall shift values

Listed here are the shifts in HS and CoG locations. ID refers to the patients' unique identifying number after anonymization, and is listed with their respective group: either "A" for the group with tumors anterior to the PrG, or "P" for those with tumors posterior to the PrG. Time interval refers to the time that elapsed between each patient's first and second mappings. The shifts, detailed as average values across either the HS or CoG shifts detected in each patient, are listed individually for the mediolateral axis (x), posteroanterior axis (y), and the resultant vector (mean 2D shift) (includes data from Conway *et al.*, 2017).

ID / group	time interval [months]	HS mean 2D shift [mm]	HS shift lxl [mm]	HS shift lyl [mm]	CoG mean 2D shift [mm]	CoG shift lxl [mm]	CoG shift lyl [mm]
1 / A	9.5	15.8	9.0	13.0	9.5	9.0	3.0
2 / A	31.0	8.2	2.0	8.0	2.7	2.7	0.7
3 / A	11.5	22.7	15.0	17.0	20.0	12.0	16.0
4 / A	18.7	22.1	2.0	22.0	24.1	6.0	23.3
5 / A	21.9	28.7	10.7	26.7	31.0	14.7	27.3
6 / A	16.0	18.1	2.0	18.0	14.0	0.7	14.0
7 / A	3.6	13.7	10.0	9.3	4.7	0.7	4.7
8 / A	10.5	8.7	8.0	3.3	4.7	4.7	0.7
9 / A	3.0	1.5	1.3	0.7	7.6	4.7	6.0
10 / A	3.6	8.1	7.3	3.3	4.7	3.3	3.3
11 / A	6.0	3.8	2.7	2.7	6.7	5.3	4.0
12 / A	5.1	6.1	1.3	6.0	4.1	0.7	4.0
13 / P	41.2	19.4	5.3	18.7	10.1	1.3	10.0
14 / P	29.7	7.1	5.0	5.0	14.1	2.0	14.0
15 / P	6.0	14.3	6.0	13.0	12.8	8.0	10.0
16 / P	15.7	17.2	10.0	14.0	11.7	6.0	10.0
17 / P	6.0	8.0	0.7	8.0	4.7	0.7	4.7
18 / P	7.2	5.1	2.0	4.7	8.1	1.3	8.0
19 / P	5.2	15.0	1.0	15.0	7.6	3.0	7.0
20 / P	6.8	19.6	6.0	18.7	15.2	6.0	14.0
21 / P	5.9	2.0	0.0	2.0	4.1	4.0	0.7
22 / P	3.0	7.8	4.0	6.7	7.5	5.3	5.3
mean	12.1	12.4	5.1	10.7	10.4	4.6	8.7
SEM	2.2	1.6	0.9	1.6	1.5	0.8	1.5
min	3.0	1.5	0.0	0.7	2.7	0.7	0.7
max	41.2	28.7	15.0	26.7	31.0	14.7	27.3
median	7.0	11.2	4.5	8.7	7.9	4.3	6.5

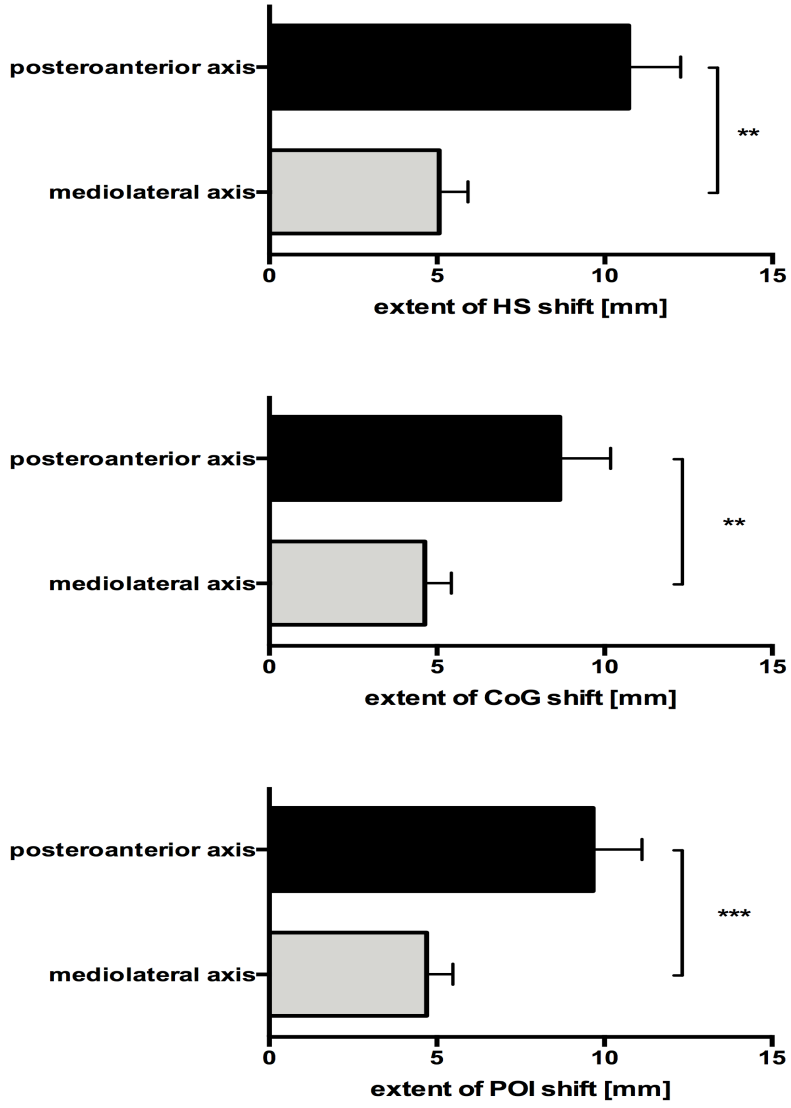

Figure 7 – average extent of shift by axis
Bar chart showing the average extent of shifts on the posteroanterior and mediolateral axes as measured in mm for HS (top graph), CoG (middle), and POI overall (bottom). The extent of shifts was found to differ significantly between the two axes in all three data sets (p=0.0011** for HS; p=0.0075** for CoG; p=0.0008*** for POI overall). SEM range is described by whiskers. The shift vectors along the cortical surface based on the presented average x and y coordinates measured an average 12.4mm ± 1.6mm in magnitude for HSs, and 10.4mm ± 1.5mm for CoGs (includes elements modified from Conway *et al.*, 2017).

3.1.2. Influence of time interval and tumor grade

Linear regression analysis of the extent of average POI shifts as a function of the time between mappings yielded a positive slope value of 0.2642 ± 0.1473 (CI -0.04298 to 0.5714) for HSs and 0.2206 ± 0.1446 (CI -0.08109 to 0.5222) for CoGs (Conway *et al.*, 2017).

This relationship between the time intervals and the positional changes of POIs was then plotted in two separate groups, formed based on tumor grade as detailed in 2.7.2. The graphs are presented in figure 8.

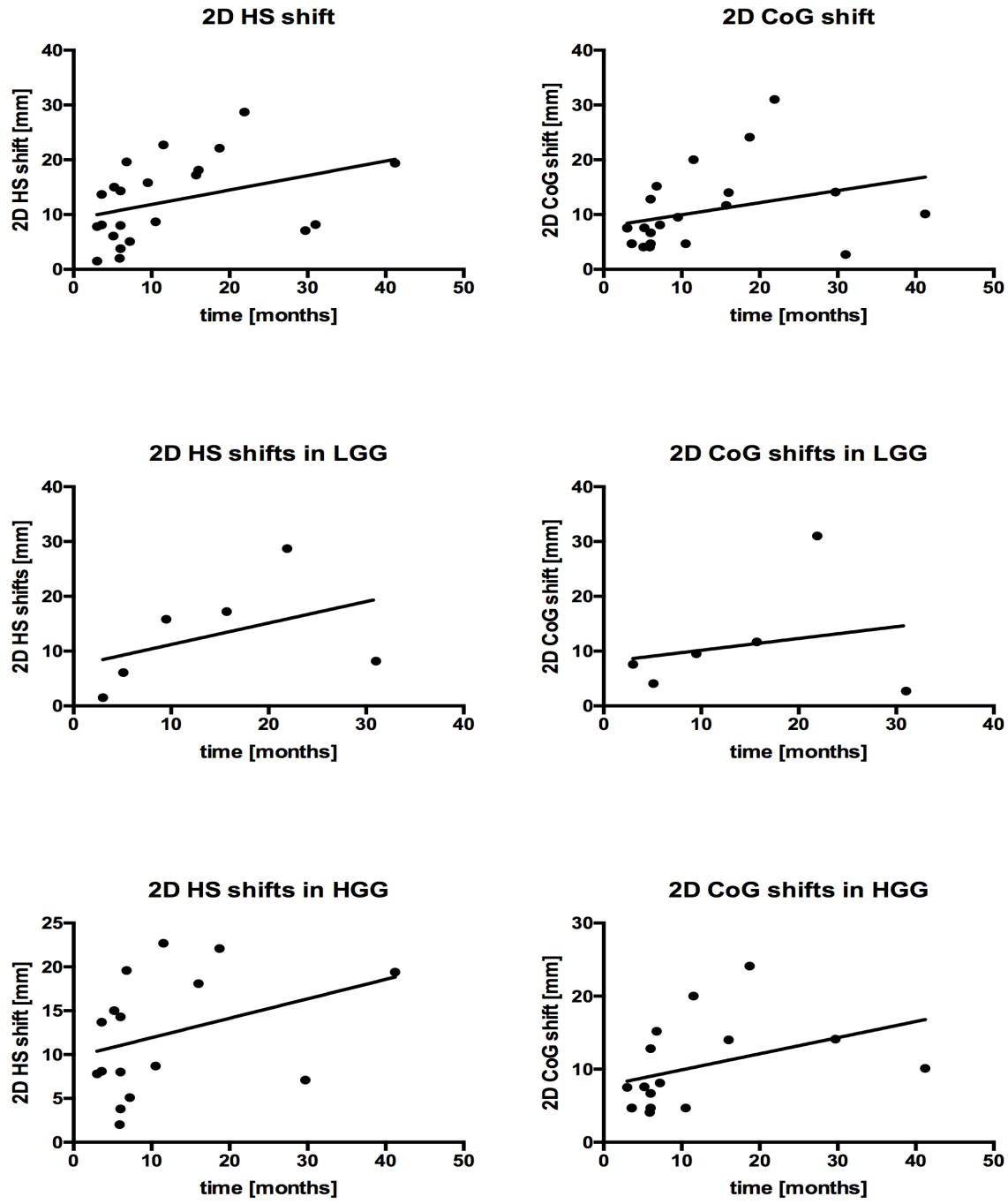

Figure 8 – 2D shift over time
These six graphs illustrate the juxtaposition of the time intervals between mappings in months on the y axes, and the average extent of shift in the locations of the POI determined at the brain surface level, in mm, on the y axis. As labeled, all graphs on the left side of the image refer to HS shifts, while those on the right show shifts registered for CoGs. While the first row includes all patients, the middle row includes only patients with LGG, and the bottom row shows the results of patients with HGG. The lines were plotted via linear regression (includes elements modified from Conway *et al.*, 2017).

3.2. Analysis of shift direction based on tumor location subgroups

Analysis of the effects of tumor location on the direction of shifts showed that POIs in group A moved by an average +4.5 ± 3.6 mm on the posteroanterior y axis, which means that, on average, they moved in an anterior direction. The opposite was true for POIs in group P, where the average shift on the y axis was calculated to be -2.6 ± 3.3 mm, which represents movement in a posterior direction. However, this difference in shift direction was not deemed statistically significant by a Mann-Whitney test (p=0.182). On the medioloateral x axis, POIs in group A shifted an average -1.9 ± 2.0 mm, while those in group P were found to have shifted by an average -0.2 ± 1.5 mm. The p value generated by a Mann-Whitney test on the difference between groups A and P with regards to shifts along the x axis was p=0.6619. For more details, see tables 3 and 4. For a visualization of all HS and CoGs by subgroup, see figure 9 (Conway *et al.*, 2017).

Table 3 – shift directions in group A
Shifts registered on each axis for HS and CoG in each patient in group A (includes data from Conway *et al.*, 2017).

ID	time interval (months)	HS-shift x (mm)	HS-shift y (mm)	CoG-shift x (mm)	CoG-shift y (mm)
1	9.5	9.0	-13.0	9.0	-3.0
2	31.0	-2.0	8.0	-2.7	0.7
3	11.5	-15.0	17.0	-12.0	16.0
4	18.7	-2.0	22.0	-6.0	23.3
5	21.9	-10.7	26.7	-14.7	27.3
6	16.0	2.0	-18.0	0.7	-14.0
7	3.6	10.0	9.3	0.7	4.7
8	10.5	-8.0	-3.3	-4.7	-0.7
9	3.0	1.3	0.7	4.7	-6.0
10	3.6	-7.3	3.3	-3.3	3.3
11	6.0	2.7	-2.7	5.3	-4.0
12	5.1	-1.3	6.0	-0.7	4.0
mean	11.7	-1.8	4.7	-2.0	4.3
SEM	2.5	2.2	3.8	2.0	3.5
min	3.0	-15.0	-18.0	-14.7	-14.0
max	31.0	10.0	26.7	9.0	27.3
median	10.0	-1.7	4.7	-1.7	2.0

Table 4 – shift directions in group P

Shifts registered on each axis for HS and CoG in each patient in group P (includes data from Conway *et al.*, 2017).

ID	time interval (months)	HS-shift x (mm)	HS-shift y (mm)	CoG-shift x (mm)	CoG-shift y (mm)
13	41.2	5.3	-18.7	-1.3	-10.0
14	29.7	-5.0	-5.0	-2.0	-14.0
15	6.0	-6.0	13.0	-8.0	10.0
16	15.7	10.0	-14.0	6.0	-10.0
17	6.0	-0.7	-8.0	0.7	-4.7
18	7.2	2.0	4.7	-1.3	8.0
19	5.2	-1.0	-15.0	-3.0	-7.0
20	6.8	-6.0	18.7	-6.0	14.0
21	5.9	0.0	-2.0	4.0	-0.7
22	3.0	4.0	-6.7	5.3	-5.3
mean	12.7	0.3	-3.3	-0.6	-2.0
SEM	4.0	1.7	3.9	1.5	3.0
min	3.0	-6.0	-18.7	-8.0	-14.0
max	41.2	10.0	18.7	6.0	14.0
median	6.4	-0.3	-5.8	-1.3	-5.0

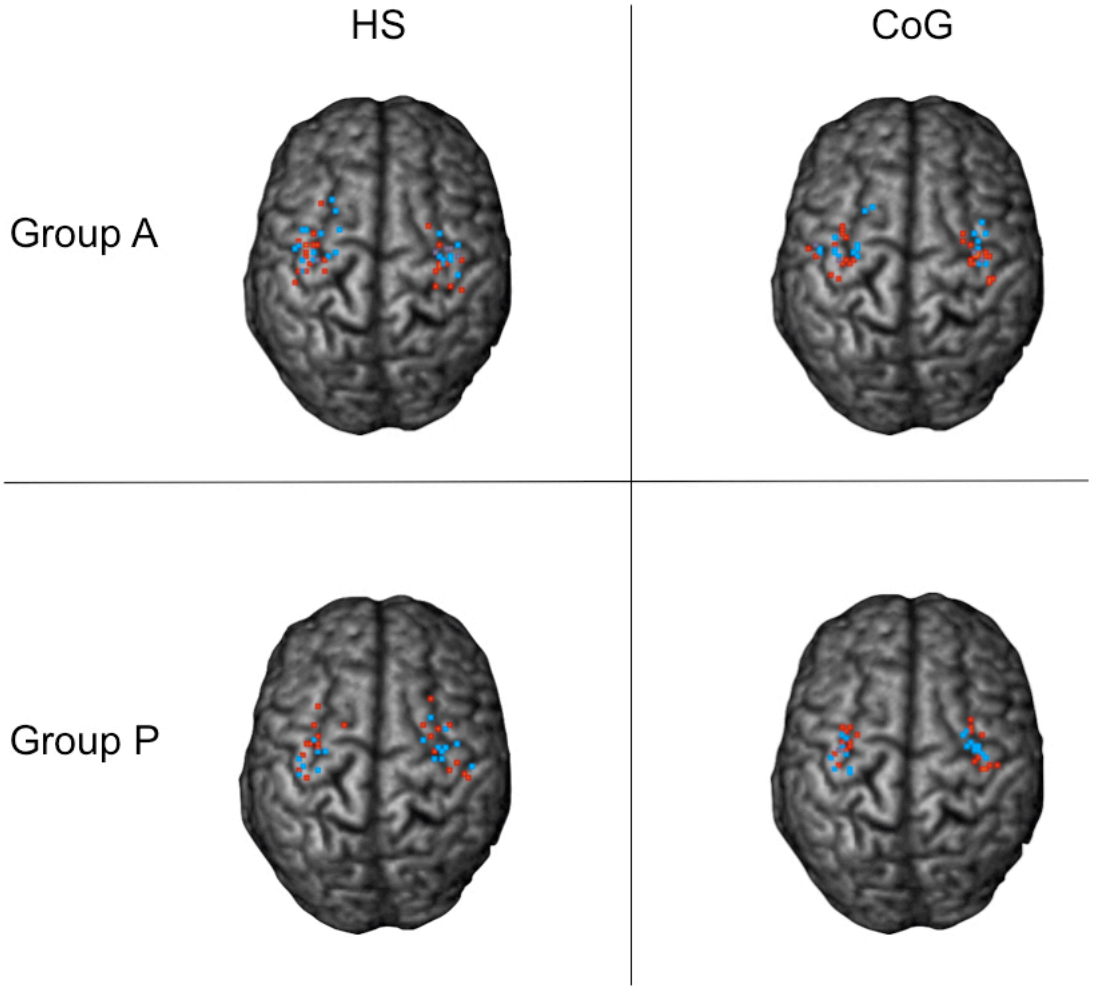

Figure 9 – HS and CoG visual overview by subgroup
A visualization of all HS and CoG locations registered across all mappings and patients. Marked in red are all points from the first mappings, with the points from the second mappings in blue. HS are visualized in the left column, with CoGs on the right. Mappings from group A are visualized in the top row, and those from group P below (modified from Conway *et al.*, 2017).

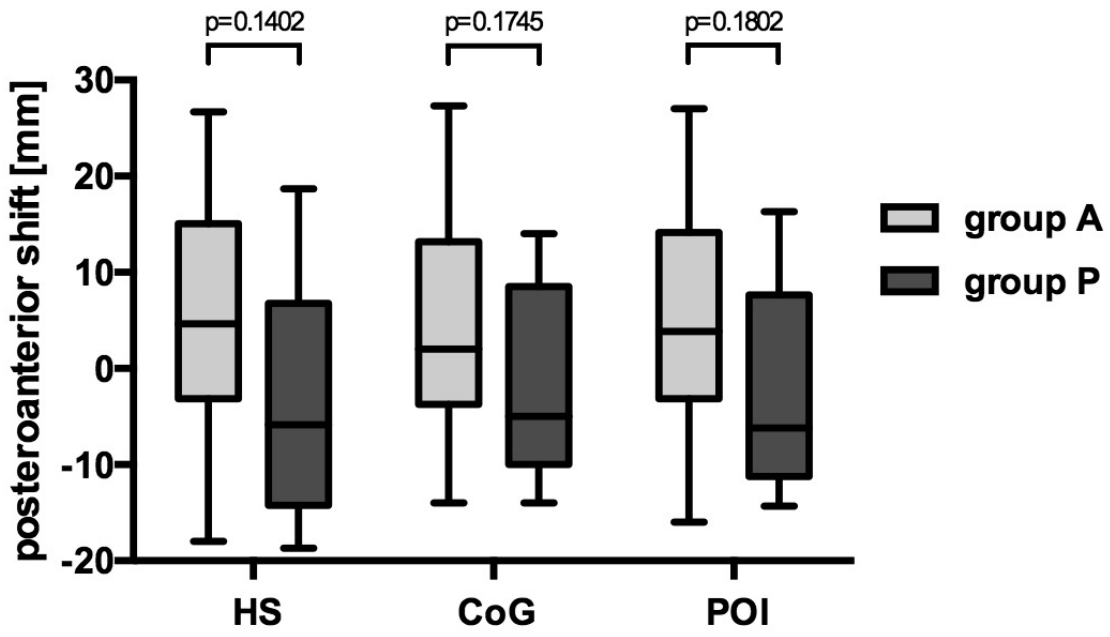

Figure 10 – shift direction by tumor location group
This candlestick chart depicts posteroanterior shifts of HS and CoG, as well as their combined average in the shape of POI. Group A and P are shown separately. Negative values on the y axis of the chart represent shifts towards posterior areas of the cortex, while positive values show that points shifted to areas anterior to their original locations. The p-values shown stem from Mann-Whitney U tests comparing groups A and P (modified from Conway *et al.*, 2017).

3.3. 10-mm count

In 11 out of 22 cases (50%), HS shifts along the cortical surface exceeded 10mm. CoG shifts exceeded 10 mm in 9 cases out of 22 (41%). Average POI shifts exceeded 10 mm in 11 cases out of 22 (50%) (Conway *et al.*, 2017).

As for the distribution of supra-threshold shifts across tumor location subgroups A and P, as well as across tumor entities, see table 2.

3.4. Visual confirmation

For an insight into how visual analysis was performed, see figure 11. No obvious discrepancies were found between the visualized raw mapping data and the results based on normalization and coordinates-based measurement. We found that edema and surgical trauma were evenly distributed across patients whose POIs demonstrated significant (at least 10 mm) positional changes, and those whose POIs remained relatively stable. As for where POIs were found to have moved to, specifically regarding their movement relative to the PrG, see table 5 (Conway *et al.*, 2017).

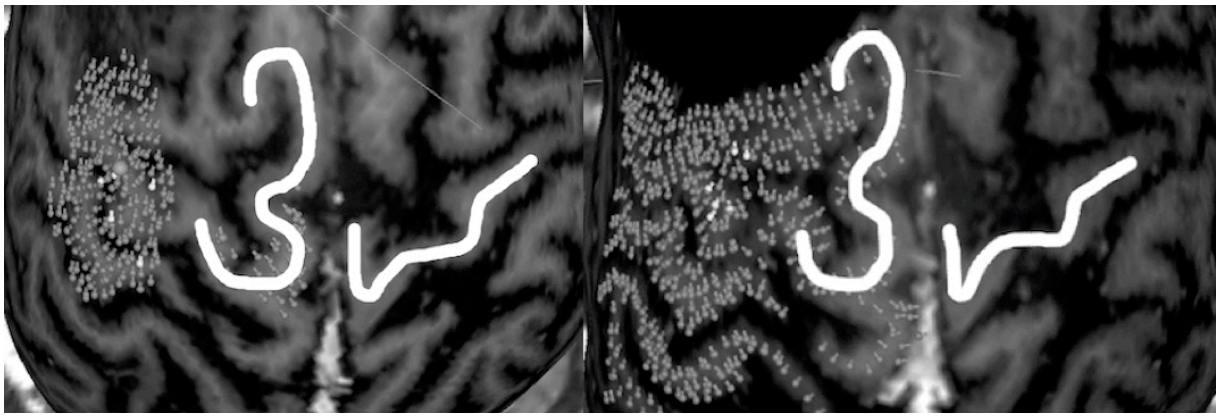

Figure 11 – visual analysis
An illustration of the visual analysis process. It consists of screenshots of 3D renderings from the first (left) and second (right) mapping session of the same patient, with the relevant POIs highlighted (white markers) among the various stimulation sites (grey markers). Adjacent gyral structures are marked with white lines for better orientation and comparison. These images are of patient ID 2. With most markers remaining within the confines of the PrG, it would appear that a slight overall shift in an anterior direction has taken place, which is in line with the calculation and coordinates-based findings (modified from Conway *et al.*, 2017).

Table 5 – visual analysis results
This table lists the anatomical tumor location as defined by the radiology department, the gyrus or gyri found to harbor motor function at the first and second mappings, as well as the visually observed direction of shifts in the position of HSs and CoGs (includes data from Conway *et al.*, 2017).

ID /group	tumor location	visually observed shift direction	HS and CoG locations map 1	HS and CoG locations map 2
1 / A	insular	towards PrG	SFG/PrG	PrG
2 / A	frontal	within PrG	PrG/PoG	PrG/MFG
3 / A	frontal	within PrG	PrG	PrG/SFG
4 / A	frontal	within PrG	PrG/PoG	PrG/MFG
5 / A	frontal	away from PrG	PrG	SFG
6 / A	frontal	towards PrG	MFG/PrG	PrG
7 / A	frontal	away from PrG	PrG	SFG/PrG
8 / A	temporal	within PrG	PrG	PrG
9 / A	frontal	towards PrG	MFG/PrG	PrG/MFG
10 / A	temporal	within PrG	PrG	PrG
11 / A	frontal	within PrG	PrG	PrG
12 / A	frontal	within PrG	PrG	PrG
13 / P	parietal	towards PrG	SFG	PrG
14 / P	parietal	towards PrG	PrG/MFG	PrG
15 / P	frontoparietal	within PrG	PrG	PrG
16 / P	parietal	within PrG	PrG/MFG	PoG/PrG
17 / P	parietal	towards PrG	MFG/PrG	PrG
18 / P	parietooccipital	within PrG	PrG	PrG
19 / P	temporal	towards PrG	SFG/PrG	PrG
20 / P	temporal	away from PrG	PrG	MFG
21 / P	parietal	within PrG	PrG	PrG
22 / P	parietal	within PrG	PrG/SFG	PrG

3.5. rMT analysis

rMT did not differ significantly between patients' first and second mappings. As for the CV, it was calculated to be 0.16. Mean rMTs at the first mappings were 35% ± 2%, mean rMTs across the second mappings were 34% ± 2%, measured as a fraction of the stimulation coil's maximum output. For a comprehensive list of rMTs across all mappings in this study, see table 6 (Conway *et al.*, 2017).

Table 6 – rMT Values
The following table lists the rMT values determined before each patients' first and second motor function mappings. The values represent a fraction of the stimulator's maximum output. For example, an rMT value of 0.20 means 20% of the maximum output were found to be the rMT for that patient's ipsilateral motor cortex at the time of mapping, and used as a basis for that mapping. A statistically significant difference between the first and second rMT values could not be shown (p=0.6430) (includes data from Conway *et al.*, 2017).

ID	rMT1	rMT2
1	0.24	0.62
2	0.59	0.49
3	0.72	0.38
4	0.35	0.36
5	0.25	0.35
6	0.43	0.37
7	0.36	0.29
8	0.37	0.35
9	0.35	0.27
10	0.26	0.24
11	0.41	0.29
12	0.33	0.37
13	0.3	0.22
14	0.28	0.29
15	0.27	0.29
16	0.32	0.32
17	0.35	0.25
18	0.3	0.47
19	0.25	0.23
20	0.27	0.3
21	0.43	0.35
22	0.26	0.3
mean	0.3	0.3
SEM	0.025	0.02
min	0.24	0.22
max	0.72	0.62
median	0.325	0.31
	p=0.6430	

4. DISCUSSION

4.1. Credibility of shifts detected

The most fundamental subject up for discussion regards the question of whether the changes remarked between POI coordinates at the first and second mappings can or should be interpreted as actual changes in the distribution of cortical motor function. Statistical testing to try and determine whether this was the case was largely inconclusive, leaving room for the argument that the observed changes were down to artifacts or the inaccuracy of our methods. While this argument cannot be totally discredited, it is also to be said that some of the statistical findings in this pilot study would appear to indicate otherwise. This is discussed in the following subsections.

4.1.1. Extent of shifts exceeds normal range of inaccuracy

It can be said that the overall degree to which POIs were found to have shifted in the presented research exceeded measurements made by previous groups analyzing the reliability of nTMS motor function mapping, which averaged 6.7 mm (Wolf *et al.*, 2004; Corneal, Butler and Wolf, 2005; Ruohonen and Karhu, 2010; McGregor *et al.*, 2012; Sollmann *et al.*, 2013; Weiss *et al.*, 2013; Forster *et al.*, 2014). It did so, however, by a fine margin.

The argument for authentic shifts becomes more credible when, instead of looking purely at the average shifts observed, one takes into account their distribution across patients. As demonstrated by particularly high SEM values, the shifts presented here were far from evenly distributed across patients, in marked contrast to the error margins in the aforementioned reliability studies. Yet, the same mapping protocol was followed, and one of those studies was performed by the same research group (Sollmann *et al.*, 2013). This may indicate that, at the very least, the more extensive shifts observed here are likely to be genuine. Given that POI shifts exceeded 10 mm in 50% of patients (HS: 50%, CoG: 41%), we conclude that, despite a likely layer of unavoidable artifacts, this points to true changes in location.

Despite clear differences between the locations of POIs between first and second mappings, rMT values remained quite constant in this study, which may be touted as another sign of accuracy in nTMS mappings (Thickbroom, Sammut and Mastaglia, 1998; Forster *et al.*, 2012, 2014).

4.1.2. Orientation of shifts as an indication

The fact that changes were significantly greater on the y axis than they were on the x axis (p=0.0008) can be seen as a further indication that the observed positional changes of POIs were bona fide (see figure 7). While not unthinkable, it seems unlikely that any non-systematic error should lead to such a result.

Looking at the literature on whether nTMS mapping might be more accurate on one axis than on the other, previous reports indicate that in the cases where this occurred, it was in fact more common for the greater variation to occur on the mediolateral axis (McGregor *et al.*, 2012; Ngomo *et al.*, 2012; Sollmann *et al.*, 2013; Forster *et al.*, 2014). A contrasting report which must be mentioned in this context found greater variation on the posteroanterior axis (Wolf *et al.*, 2004). Seeing as that study, however, used TMS without MRI navigation, we would argue that it is outweighed by the reports previously mentioned.

As for shift direction relative to the tumor site, it is noteworthy that the overall average shift direction in group A was anterior, while group P averaged shifts in a posterior direction. Though this difference between groups was not statistically significant, it does indicate that the shifts seem to follow a pattern, as opposed to being the product of random inaccuracy. POI shifts towards the resection cavity – as observed here – can be seen as supporting the theory that the driving force behind these shifts was functional reorganization of the motor cortex. While the surgical team aimed to avoid resection of motor positive stimulation points, it remains a strong possibility that some were either resected or otherwise adversely affected by surgery. Even if these areas were not the sites of POIs in and of themselves, their removal could certainly affect CoG calculation, seeing as CoG calculation is based on a series of stimulation sites. If one such site were to be resected, this would then result in a shift of the corresponding CoG. Such a shift would, however, be directed away from the resection cavity, or mask a wider shift of motor function towards it. So if this effect did take place, it seems to have been outweighed by an overall relocation of motor function in the opposite direction (towards the resection cavity).

Shifts in an anterior direction have previously been reported in stroke patients after stimulation (Liepert *et al.*, 1998; Byrnes *et al.*, 2001), and, in individual cases, during or after glioma surgery (Duffau, 2001; Forster *et al.*, 2012).

4.1.3. Methodological limitations

One source of inaccuracy is of course the procedure of nTMS mapping itself. As detailed above, the extent of inaccuracy in repeat nTMS motor mappings has been described as measuring an approximate 6.7 mm (Wolf *et al.*, 2004; Corneal, Butler and Wolf, 2005;

Ruohonen and Karhu, 2010; McGregor *et al.*, 2012; Sollmann *et al.*, 2013; Weiss *et al.*, 2013; Forster *et al.*, 2014). This led to the application of a 10 mm cut-off count in this study, which 50% of observed POI shifts exceeded.

As glioma patients often present with secondary edema and scarring of the cortex these are further factors that might be expected to have adverse effects on nTMS readings. A previous study was, however, able to show that these effects are largely negligible (Krieg *et al.*, 2013). To compensate for possible mass effect of tumors during the first, and the shifting of brain tissue toward the resection matter in the second mappings, cost-function masking was used to help with the normalization of our images. Seeing as it alters the MR images upon which our measurements are based, the normalization process is of course a possible source of distortion (Brett *et al.*, 2001; Andersen, Rapcsak and Beeson, 2010).

Lastly, visual analysis is always dependent on the observer, which makes it somewhat unreliable. For this reason, it was only used as a means of double-checking the results obtained by arithmetic means.

4.1.4. Observations on sample size

Given that the presented study included only 22 patients, and given the subtle nature of the effects it was aimed at observing, sample size would appear its most significant limitation. It limits the extent to which conclusions can be drawn from the results, as demonstrated by the many findings that did not reach statistical significance, hence rendering attempts at extrapolating the wider patterns at play inconclusive. However, data from our study can help provide information on the expected frequency of shifts of HS and CoG occurring in glioma patients peri- or postoperatively. We found that HS shifts exceeded 10 mm in 50% of patients, and CoG shifts did so in 41%. As detailed above, it appears reasonable to assume that shifts of this magnitude are unlikely to merely represent artifacts or inaccuracy.

4.1.5. Further limitations specific to this study

A further structural shortcoming of the study was the variation of follow-up periods between mappings. Future studies should consider setting stricter limits for the minimum and maximum time allowed to elapse between the first mapping and the second. It might also prove helpful to conduct more than two mappings, patient survival and compliance allowing.

There is also virtue to the argument that the model of this study contains two potentially conflicting interventions: tumor resection on one hand, and potential recurrence, or continued expansion of remaining cancerous tissue, on the other. Yet this can hardly be avoided.

Studies with glioma patients not undergoing surgical treatment would be of interest for comparison, but seeing as surgery is considered the first line of treatment, patient recruitment would prove difficult.

Plastic potential is often found to be greater in patients with LGG as opposed to higher grade, more quickly developing malignancies (Duffau *et al.*, 2003). Future studies, with larger cohorts, should consider analyzing subgroups by tumor entity, i.e. WHO grade. Due to the limited sample size in this study, our efforts in this regard were inconclusive.

4.2. Interpreting the observations

Working on the premise that changes of POI positions were accurately registered, the question remains as to how these changes can be explained, and how they might impact our understanding of lesion-induced cortical reorganization. As referenced in the introduction, Hugues Duffau and colleagues had the opportunity to observe a phenomenon dubbed acute "unmasking" of motor sites upon resection of a perirolandic glioma (Duffau, 2001, 2014b). In line with our findings, the shift direction observed in that case was towards the resection cavity. In their discussion of this much-cited instance, the authors deduced that the unmasked motor sites had most likely been muted by the tumor's mass effect, leading to their re-activation upon its removal. Much the same reasoning could be applied to explain the shifts detected in our study. As magnetoencephalography studies have suggested, peritumoral edema can have an inhibitory effect on cognitive function in the grey matter affected (Fernández-Bouzas *et al.*, 1997; Douw *et al.*, 2008). Such an inhibition, developed over the course of the tumors' growth, could therefore plausibly have inhibited adjacent motor cortex. Upon subsequent resection of the tumor, it would then appear that this inhibition may have ended, resulting in a return of primary motor function to its original location by re-activation. The fact that out of the 17 patients in our cohort that presented without motor deficit at the time of their first preoperative nTMS mapping, 9 showed an average shift of HSs and CoGs above the 10mm threshold, seems to fit this explanation: in order to preserve motor function despite the impairment of parts of the PrG, alternative areas more distant to the tumor might have been recruited in the period of tumor growth preceding the first motor mapping.

When it comes to alternative sites lesioned brains have been known to reroute primary motor function to, they are generally placed into three categories: Ipsilateral areas near the ones hitherto responsible, and within the PrG; Ipsilateral, slightly more remote sites in adjacent gyri; and in the corresponding parts of the contralateral hemisphere (Weiller, 1998; Rijntjes and Weiller, 2002; Heiss *et al.*, 2003; Krainik *et al.*, 2004; Duffau, 2005; Sandrini and Cohen, 2013). While the contralateral hemispheres were not examined in our study, we paid explicit

attention to extensively explore not just the PrG, but also the SFG, MFG and PoG for MEP-eliciting sites during our repeat nTMS motor mappings, given evidence that all of these areas may contain direct corticospinal projections (Dum and Strick, 2002; Teitti *et al.*, 2008). Another project by our research group was able to confirm the presence of short-latency primary motor function in these areas in tumor patients, further underlining their importance to functional compensation in glioma patients (Bulubas *et al.*, 2016). It therefore seems likely that the shift of MEP sites back towards the resection cavity observed in our study followed an initial shift away from the growing tumor to adjacent areas, both within and beyond the confines of the PrG.

Alternatively, the motor function maps drawn by our preoperative mappings might not have contained additional MEP sites relative to the patients' functional anatomy before the onset of glioma. Instead, the observed shifts could simply be the result of the original distribution of function being – at least partially – restored, but without prior recruitment of additional circuits. This possibility is, of course, impossible to discount, given the unavailability of data on our patients from before they presented with glioma. Even the apparent lack of deficit in such a large number of patients may be explained by difficulties in registering subtle, complex deficits. However, the motor cortex' capacity to perform to a comparatively normal standard despite a portion of its key areas being muted is already a demonstration of functional reorganization, likely based on the de-inhibition of pre-existing redundant pathways, a commonly postulated mechanism (Jacobs and Donoghue, 1991; Duffau, Sichez and Lehéricy, 2000).

4.3. Surgical implications

If glioma resection can encourage a return of primary motor function towards the resection cavity, subtotal resection as part of a multi-stage surgical strategy as has been proposed (Martino *et al.*, 2009; Duffau and Taillandier, 2015) may effectively alleviate the tumor's mass effect. That could bear the risk of reducing the driving force for compensatory reorganization this approach relies on for preserving motor function. As seen in reported cases of successful, function-preserving multi-stage surgery, this need not always be the case (Gil Robles *et al.*, 2008; Takahashi *et al.*, 2012). However, given the shifts of primary motor function in the direction of the resection cavity seen in our study, one might suggest that such possibly counter-productive effects be kept in mind. This could add further strength to the argument for maximizing EOR. GTR has already been shown to improve outcome for both LGG and HGG (Sanai and Berger, 2011; Suchorska *et al.*, 2016), with some even promoting supratotal resection as the way forward for LGG surgery (Schucht *et al.*, 2014, 2015). The pathophysiological argument for this approach is compelling: resecting beyond the margins

of the tumor as defined by MRI contrast enhancement reduces the likelihood of residual tumor cells, as yet indiscernible from healthy tissue, remaining in situ. In turn, the likelihood of recurrence and subsequent malignant transformation are reduced (Yordanova and Duffau, 2017).

The limiting factor when seeking to maximize EOR is of course the integrity of functionally eloquent brain. Here, nTMS can play a vital role in the planning of surgery, particularly with regards to prefrontal areas that might traditionally be deemed expendable. Our research group was able to demonstrate the correlation of permanent paresis and the removal of motor-positive stimulation sites (Moser *et al.*, 2017). Another of our projects showed the potential benefits for individual risk assessment of nTMS-seeded DTI fiber tracking (Sollmann, Wildschuetz, *et al.*, 2018).

The complexity of the apparent trade-off between motor function and tumor resection, however, was further highlighted by another study conducted by our group. It showed that glioma tend to grow towards eloquent cortex, and indicated that prioritizing short-term preservation of function may actually be disadvantageous not only from an oncological perspective, but also with regards to medium-term function preservation and quality of life (Sollmann, Laub, *et al.*, 2018).

Taken together with the indications from the present study that primary motor function might shift back towards the resection cavity – and possible tumor recurrence –we believe that the case for maximizing EOR while using nTMS motor mapping in combination with DTI fiber tracking as a reference has been strengthened.

Besides planning for surgery, nTMS may also have a role to play in deciding on the ideal timing of surgery. It would appear possible that in patients whose positive mapping points are initially very close to or within the tumor, delaying surgery to allow time for a possible redistribution could be a viable option. With repeat mappings, such a redistribution could be recognized to help decide on the right time for the delayed resection.

4.4. Limitations

As mentioned in section 4.1., there are a number of limitations to consider when weighing the results and possible ramifications of this study. nTMS motor mapping is an established method, but does of course bear inherent inaccuracies due to the imaging and neuronavigation it relies upon. Further distortions may also have been caused by the normalization process which our images underwent to enhance comparability and attempt to account for tumor mass effect. Also, visual analysis, though used here only as an additional safeguard, is of course subjective by nature.

This study's sample size was small. While not unusual in studies on severely impairing, lethal disease such as high-grade glioma, this might reduce the power of this study and could limit the extent to which conclusions ought to be drawn from it.

Follow-up periods varied from patient to patient, largely for logistical and patient-specific reasons. Furthermore, it is not possible to definitively determine the main cause for functional reorganization observed in this study, due to the concomitant occurrence of two possible drivers: tumor growth and tumor resection.

Any clinical decisions taken based on the present study need to be taken with these significant limitations in mind. Further studies are needed to conclusively solidify or disprove its findings.

5. CONCLUSION

This study was able to demonstrate changes in the distribution of motor function in glioma patients along the posteroanterior axis of the motor cortex. These changes were significantly greater than any changes found on the mediolateral axis, which may support the conclusion that they were a genuine sign of functional reorganization of the motor cortex.

The methods described in this dissertation therefore seem suitable for the detection and monitoring of functional reorganization in post-surgical glioma patients, though improvements remain to be made. We observed positional changes above the threshold level of 10 mm, and thus suggesting functional reorganization, in 9 out of 22 patients when analyzing for HS shifts, and in 11 out of 22 cases when analyzing for CoG shifts.

It appears that, in line with previous findings in similar settings, functional reorganization seen in this study consisted mainly of cortical redistribution of motor function back towards the glioma resection cavity, though the level to which this is the norm needs to be evaluated further.

Though this effect was not statistically significant, it may be viewed as a further indication that maximizing EOR is a necessary step towards preserving motor function in the longer term, lest the reorganization caused by tumor growth be reversed.

6. OUTLOOK

Several improvements to the performed study should be applied to any future projects aimed at further establishing or rejecting these methods, and verifying our findings. First and foremost amongst these improvements is sample size, which in retrospect was not sufficient here. An added benefit of increased sample size would be the possibility of sufficiently large subgroups based on tumor grade. Our estimation that true HS shifts were found in at least 50% of patients, and true CoG shifts in at least 41% of patients, although based on just 22 patients, may help power future studies.

Future studies should also include mappings at fixed time intervals, and use at least one additional mapping immediately postoperatively. When comparing such a postoperative mapping with later mappings, researchers might also be able to avoid the need for cost-function masking to account for the removal of the tumor between mappings, thereby circumventing the uncertainty regarding its adequacy in this context.

The significance of nTMS as a tool for both clinical use and research remains unchanged. It appears to be a uniquely non-invasive way of identifying functional reorganization in the motor cortex, and should undergo further exploration in this context.

7. SUMMARIES

7.1. English

Introduction: Navigated transcranial magnetic stimulation (nTMS) is a reliable instrument for the non-invasive localization of primary motor function in the human cortex. Due to the frequency with which gliomas affect the motor cortex, or grow towards it, nTMS is already widely used for planning glioma resection surgery. It is often observed that glioma patients develop little or no motor deficit despite the motor cortex being heavily affected or even altered by the tumor. This lack of deficit can often be attributed to functional reorganization of the cortex. The goal of this study was to evaluate nTMS as a tool for observing such reorganization in patients suffering from glioma in the vicinity of the precentral gyrus (PrG). Furthermore, we aimed to draw preliminary conclusions regarding the frequency of such changes, and discernible patterns regarding the direction or timing of such reorganization in order to help facilitate future studies.

Methods: To this end, 22 patients suffering from glioma near the PrG were recruited. Mappings of the motor cortex were conducted using nTMS both before, and 3-42 months after glioma resection surgery. To better compare pre- and postoperative mappings, the hotspots (HS) and centers of gravity (CoG) of each mapping were determined, and the imaging data was subjected to normalization to account for orientation and physical effects of the surgery. To estimate the frequency of significant shifts of primary motor function, we determined in how many cases HS or CoG shifted by more than 10 mm on the cortical surface. To analyze the possible role of tumor position in determining redistribution patterns, patients were also analyzed in subgroups based whether their tumor was found to be mainly anterior (Group A) or posterior (Group P) to the PrG.

Results: We found an average shift of HS by 5.1 mm ± 3.3 mm SEM on the mediolateral axis, and 10.7 mm ± 1.6 mm SEM on the anteroposterior axis. CoG moved by an average 4.6 mm ± 0.8 mm SEM on the mediolateral, and 8.7 mm ± 1.5 mm SEM on the anteroposterior axis. Shifts on the anteroposterior axis were thus found to be significantly greater than the changes observed on the mediolateral axis. In Group A, HS and CoG averaged an anterior shift of 4.5 mm ± 3.6 mm SEM, while the average shift in Group P was posteriorward, 2.6 ± 3.3 mm SEM. Overall, out of 22 patients, HS shifts were greater than 10 mm in 11 cases, while CoG shifts exceeded that value in 9 patients.

Conclusions: The methods described here appear suitable for the detection and monitoring of motor cortical functional reorganization in glioma patients, though improvements remain to be made. On average, the shifts detected here were oriented back towards the resection cavity. However, further studies are needed to determine whether this pattern represents the norm. These studies should include a range of improvements, most importantly including larger sample size. If confirmed, the results from this study may be another argument in favor of maximizing the extent of resection through an aggressive resection strategy supported by nTMS.

7.2. Deutsch

Einführung: Die navigierte transcranielle Magnetstimulaton (nTMS) ist eine Methode, mit der sich zuverlässig und nichtinvasiv die Positionen von für die Ausführung von Bewegungen relevanten Hirnrindenneuronen bestimmen lassen. nTMS wird bereits vielfach zur Planung von neurochirurgischen Eingriffen bei Gliompatienten verwendet, da Gliome häufig in der Nähre relevanter kortikaler Areale entstehen, oder auf diese zuwachsen. Es wird häufig beobachtet, dass Gliompatienten keine oder wenige motorische Defizite aufweisen, obwohl der Tumor den motorischen Kortex massiv affektiert. Dies wird in vielen Fällen auf kortikale funktionelle Reorganisation zurückgeführt. Ziel der vorliegenden Studie war es, nachzuvollziehen inwiefern sich nTMS als Instrument eignet, um solche kortikale funktionelle Reorganisation bei Gliompatienten mit Tumoren im Bereich des motorischen Kortex zu erfassen. Außerdem sollten zugunsten möglicher zukünftiger Studien vorläufige Aussagen über die Häufigkeit solcher Veränderungen, sowie über dabei möglicherweise erkennbare Muster getroffen werden.

Methoden: Es wurden 22 Patienten mit Gliomen in der Nähe des Gyrus präcentralis rekrutiert. Bei jedem Patienten wurde sowohl prä-operativ, als auch zwischen 3 und 42 Monate nach Gliomresektion jeweils eine Kartierung des motorischen Kortex mittels nTMS angefertigt. Um die beiden Kartierungen vergleichen zu können, wurden die üblichen Messpunkte „Hotspot“ (HS) und „Center of Gravity“ (CoG) bestimmt. Daraufhin wurden die Bilddaten vor der Messung einer sogenannten „Normalisierung“ unterzogen, um die Ausrichtung im Koordinatensystem zu eichen und die Masseneffekte des Tumors, beziehungsweise seiner Resektion, zu kompensieren. Anhand der genormten Bilddaten konnte nun abgemessen werden, wie weit die HS und CoG bei der zweiten Kartierung von ihrer ursprünglichen Position entfernt waren. sich zwischen den beiden Kartierungen entlang der Kortexoberfläche verschoben hatten. Um die Häufigkeit Signifikanter Verschiebungen abschätzen zu können, wurde ermittelt, wie häufig eine Verschiebung um über 10 mm auf der Kortexoberfläche feststellbar war. Des Weiteren wurde untersucht, ob sich die Position des Tumors im Vergleich zum motorischen Kortex auf die Richtung der Umverteilung ausgewirkt hatte. Hierzu wurden die Patienten in zwei Gruppen eingeteilt, je nachdem ob sich ihr Tumor anterior (Gruppe A) oder posterior (Gruppe P) des Gyrus präcentralis befand.

Ergebnisse: Es wurde eine durchschnittliche Verschiebung von HS um 5,1 mm ± 3,3 mm Standardfehler (SEM) auf der mediolateralen Achse, und 10,7 mm ± 1,6 mm SEM auf der anteroposterioren Achse festgestellt. CoG verschoben sich im Mittel um 4,6 mm

± 0,8 mm SEM auf der mediolateralen, sowie 8,7 mm ± 1,5 mm SEM auf der antero-posterioren Achse. Verschiebungen auf der anteroposterioren Achse waren somit signifikant größer als die auf der mediolateren Achse gemessenen Veränderungen. Bei Patienten mit anterior gelegenen Gliomen bewegten sich die Punkte im Mittel 4,5 mm ± 3,6 mm SEM nach anterior, bei posterior gelegenen Tumoren 2,6 mm ± 3,3 mm SEM nach posterior. Insgesamt bewegten HS sich in 11 von 22 Fällen um mehr als 10 mm, bei CoG war das bei 9 von 22 Patienten der Fall.

Schlussfolgerungen: Die hier beschriebenen Methoden scheinen geeignet zu sein für das Erfassen und Mitverfolgen von motorisch-kortikaler funktioneller Reorganisation bei Gliompatienten, auch wenn an einigen Stellen Verbesserungen vorgenommen werden sollten. In dieser Studie wurde durchschnittlich eine Rückverlagerung der primären motorischen Kortexareale hin zur Resektionshöhle festgestellt. Um festzustellen, ob es sich dabei um einen generellen Trend handelt, sind jedoch weitere Studien erforderlich. Diese sollten an einigen Stellen Verbesserungen beinhalten, allen voran eine größere Stichprobe an Patienten. Sollte sich dieses Ergebnis bestätigen, mag es als ein weiteres Argument betrachtet werden für eine aggressive Tumorresektionsstrategie unter Zuhilfenahme von nTMS.

8. FIGURES

9. TABLES

10. REFERENCES

Ahdab, R. *et al.* (2010) “Comparison of ‘standard’ and ‘navigated’ procedures of TMS coil positioning over motor, premotor and prefrontal targets in patients with chronic pain and depression,” *Neurophysiologie Clinique/Clinical Neurophysiology*, 40(1), pp. 27–36. doi: 10.1108/02686901011069560.

Andersen, S. M., Rapcsak, S. Z. and Beeson, P. M. (2010) “Cost function masking during normalization of brains with focal lesions: Still a necessity?,” *NeuroImage*. Elsevier Inc., 53(1), pp. 78–84. doi: 10.1016/j.neuroimage.2010.06.003.

Awiszus, F. and Feistner, H. (2007) “Kortikale Reizschwelle,” in Siebner, H. R. and Ziemann, U. (eds.) *Das TMS-Buch: Handbuch der transkraniellen Magnetstimulation*. Berlin, Heidelberg: Springer Berlin Heidelberg, pp. 149–158. doi: 10.1007/978-3-540-71905-2_14.

Barker, A. T., Jalinous, R. and Freeston, I. L. (1985) “Non-invasive magnetic stimulation of human motor cortex,” *The Lancet*. Elsevier, 325(8437), pp. 1106–1107. doi: 10.1016/S0140-6736(85)92413-4.

Berlucchi, G. and Buchtel, H. A. (2009) “Neuronal plasticity: Historical roots and evolution of meaning,” *Experimental Brain Research*, 192(3), pp. 307–319. doi: 10.1007/s00221-008-1611-6.

Brasil-Neto, J. P. *et al.* (1992) “Topographic mapping of the human motor cortex with magnetic stimulation: factors affecting accuracy and reproducibility.,” *Electroencephalography and clinical neurophysiology*, 85(1), pp. 9–16.

Brett, M. *et al.* (2001) “Spatial normalization of brain images with focal lesions using cost function masking.,” *NeuroImage*, 14, pp. 486–500. doi: 10.1006/nimg.2001.0845.

Brodmann, K. (1909) “Vergleichende Lokalisationslehre der Großhirnrinde: in ihren Prinzipien dargestellt auf Grund des Zellenbaues,” *Johann Ambrosius Barth, Leipzig*. doi: 10.1097/00005053-191012000-00013.

Bucur, M. and Papagno, C. (2018) “A systematic review of noninvasive brain stimulation for post-stroke depression,” *Journal of Affective Disorders*, pp. 69–78. doi: 10.1016/j.jad.2018.05.026.

Bulubas, L. *et al.* (2016) “Motor areas of the frontal cortex in patients with motor eloquent brain lesions.,” *Journal of Neurosurgery*, (April), pp. 1–12. doi: 10.3171/2015.11.JNS152103.

Byrnes, M. L. *et al.* (2001) “Long-term changes in motor cortical organisation after recovery from subcortical stroke,” *Brain Research*, 889(1–2), pp. 278–287. doi: 10.1016/S0006-8993(00)03089-4.

Chang, D. *et al.* (2018) “Smoking Cessation With 20 Hz Repetitive Transcranial Magnetic Stimulation (rTMS) Applied to Two Brain Regions: A Pilot Study,” *Frontiers in Human Neuroscience*, 12, p. 344. doi: 10.3389/fnhum.2018.00344.

Chouinard, P. A. and Paus, T. (2006) “The Primary Motor and Premotor Areas of the Human Cerebral Cortex,” *The Neuroscientist*, 12(2), pp. 143–152. doi: 10.1177/1073858405284255.

Classen, J. (2013) “Plasticity,” in Lozano, A. M. and Hallett, M. (eds.) *Handbook of clinical neurology*. Elsevier, pp. 525–534. doi: 10.1016/B978-0-444-53497-2.00041-3.

Cohen, L. G. *et al.* (1990) “Effects of coil design on delivery of focal magnetic stimulation. Technical considerations,” *Electroencephalography and Clinical Neurophysiology*, 75(4), pp. 350–357. doi: 10.1016/0013-4694(90)90113-X.

Conforto, A. B. *et al.* (2004) “Impact of coil position and electrophysiological monitoring on determination of motor thresholds to transcranial magnetic stimulation,” *Clinical Neurophysiology*, 115(4), pp. 812–819. doi: 10.1016/j.clinph.2003.11.010.

Conway, N. *et al.* (2017) “Cortical plasticity of motor-eloquent areas measured by navigated transcranial magnetic stimulation in patients with glioma,” *Journal of Neurosurgery*, 127(5), pp. 981–991. doi: 10.3171/2016.9.JNS161595.

Corneal, S. F., Butler, A. J. and Wolf, S. L. (2005) “Intra- and intersubject reliability of abductor pollicis brevis muscle motor map characteristics with transcranial magnetic stimulation,” *Archives of Physical Medicine and Rehabilitation*, 86(8), pp. 1670–1675. doi: 10.1016/j.apmr.2004.12.039.

D’Amico, R. S. *et al.* (2017) “Extent of Resection in Glioma–A Review of the Cutting Edge,” *World Neurosurgery*. Elsevier Inc, 103, pp. 538–549. doi: 10.1016/j.wneu.2017.04.041.

Dayan, E. and Cohen, L. G. (2011) “Neuroplasticity subserving motor skill learning,” *Neuron*, 72(3), pp. 443–454. doi: 10.1016/j.neuron.2011.10.008.

DeAngelis, L. M. (2001) “Brain Tumors,” *The New England Journal of Medicine*, 344(2), pp. 114–123. doi: 10.1227/01.NEU.0000311254.63848.72.

Defrin, R. *et al.* (2007) “The effect of a series of repetitive transcranial magnetic stimulations of the motor cortex on central pain after spinal cord injury.,” *Archives of physical medicine and rehabilitation*, 88(12), pp. 1574–80. doi: 10.1016/j.apmr.2007.07.025.

Dong, X. *et al.* (2018) “Repetitive transcranial magnetic stimulation for the treatment of Alzheimer’s disease: A systematic review and meta-analysis of randomized controlled trials,” *PLOS ONE*. Edited by K. Chen, 13(10), p. e0205704. doi: 10.1371/journal.pone.0205704.

Douw, L. *et al.* (2008) “Treatment-related changes in functional connectivity in brain tumor patients: A magnetoencephalography study,” *Experimental Neurology*, 212(2), pp. 285–290. doi: 10.1016/j.expneurol.2008.03.013.

Draganski, B. *et al.* (2004) “Changes in grey matter induced by training,” *Nature*, 427(6972), pp. 311–312. doi: 10.1038/427311a.

Duffau, H. (2001) “Acute functional reorganisation of the human motor cortex during resection of central lesions: a study using intraoperative brain mapping.,” *Journal of Neurology, Neurosurgery & Psychiatry*, 70(4), pp. 506–513. doi: 10.1136/jnnp.70.4.506.

Duffau, H. *et al.* (2003) “Functional recovery after surgical resection of low grade gliomas in eloquent brain: Hypothesis of brain compensation,” *Journal of Neurology, Neurosurgery & Psychiatry*, 74(7), pp. 901–907. doi: 10.1136/jnnp.74.7.901.

Duffau, H. *et al.* (2005) “Contribution of intraoperative electrical stimulations in surgery of low grade gliomas: A comparative study between two series without (1985-96) and with (1996-2003) functional mapping in the same institution,” *Journal of Neurology, Neurosurgery & Psychiatry*, 76(6), pp. 845–851. doi: 10.1136/jnnp.2004.048520.

Duffau, H. (2005) “Lessons from brain mapping in surgery for low-grade glioma : insights into associations between tumour and brain plasticity,” *The Lancet Neurology*, 4(August), pp. 476–486.

Duffau, H. (2014a) “Surgical neurooncology is a brain networks surgery: A ‘connectomic’ perspective,” *World Neurosurgery*. Elsevier Inc, 82(3), pp. e405–e407. doi: 10.1016/j.wneu.2013.02.051.

Duffau, H. (2014b) “The huge plastic potential of adult brain and the role of connectomics: New insights provided by serial mappings in glioma surgery.,” *Cortex*. Elsevier Ltd, 58, pp. 325–337. doi: 10.1016/j.cortex.2013.08.005.

Duffau, H., Denvil, D. and Capelle, L. (2002) “Long term reshaping of language, sensory, and motor maps after glioma resection: a new parameter to integrate in the surgical strategy.,” *Journal of Neurology, Neurosurgery & Psychiatry*, 72(4), pp. 511–6. doi: 10.1136/jnnp.72.4.511.

Duffau, H., Sichez, J. P. and Lehéricy, S. (2000) “Intraoperative unmasking of brain redundant motor sites during resection of a precentral angioma: Evidence using direct cortical stimulation,” *Annals of Neurology*, 47(1), pp. 132–135. doi: 10.1002/1531-8249(200001)47:1<132::AID-ANA23>3.0.CO;2-0.

Duffau, H. and Taillandier, L. (2015) “New concepts in the management of diffuse low-grade glioma: Proposal of a multistage and individualized therapeutic approach,” *Neuro-Oncology*, 17(3), pp. 332–342. doi: 10.1093/neuonc/nou153.

Dum, R. P. and Strick, P. L. (2002) “Motor areas in the frontal lobe of the primate,” *Physiology & Behavior*, 77(4), pp. 677–682. doi: https://doi.org/10.1016/S0031-9384(02)00929-0.

Ettinger, G. J. *et al.* (1998) “Experimentation with a transcranial magnetic stimulation system for functional brain mapping,” *Medical Image Analysis*, 2(2), pp. 133–142. doi: 10.1016/S1361-8415(98)80008-X.

Fernández-Bouzas, A. *et al.* (1997) “Evolution of cerebral edema and its relationship with power in the theta band,” *Electroencephalography and Clinical Neurophysiology*, 102(4), pp. 279–285. doi: 10.1016/S0013-4694(96)96049-6.

Foerster, O. (1936) “The motor cortex in man in the light of Hughlings Jackson’s doctrines,” *Brain*, 59(2), pp. 135–159. doi: 10.1093/brain/59.2.135.

Forst, D. A. *et al.* (2014) “Low-Grade Gliomas,” *The Oncologist*, 19(4), pp. 403–413. doi: doi:10.1634/theoncologist.2013-0345.

Forster, M.-T. *et al.* (2011) “Navigated transcranial magnetic stimulation and functional magnetic resonance imaging: Advanced adjuncts in preoperative planning for central region tumors,” *Neurosurgery*, 68(5), pp. 1317–1324. doi: 10.1227/NEU.0b013e31820b528c.

Forster, M.-T. *et al.* (2012) “Motor cortex evaluation by ntms after surgery of central region tumors: A feasibility study,” *Acta Neurochirurgica*, 154, pp. 1351–1359. doi: 10.1007/s00701-012-1403-4.

Forster, M.-T. *et al.* (2014) “Test-retest reliability of navigated transcranial magnetic stimulation of the motor cortex.,” *Neurosurgery*, 10 Suppl 1, pp. 51–56. doi: 10.1227/NEU.0000000000000075.

Fregni, F. *et al.* (2005) “Non-invasive brain stimulation for Parkinson’s disease: A systematic review and meta-analysis of the literature,” *Journal of Neurology, Neurosurgery and Psychiatry*, pp. 1614–1623. doi: 10.1136/jnnp.2005.069849.

Giglhuber, K. *et al.* (2017) “Evoking visual neglect-like deficits in healthy volunteers - an investigation by repetitive navigated transcranial magnetic stimulation.,” *Brain Imaging and Behavior*, 11(1), pp. 17–29. doi: 10.1007/s11682-016-9506-9.

Gil Robles, S. *et al.* (2008) “Long-term brain plasticity allowing a multistage surgical approach to World Health Organization Grade II gliomas in eloquent areas.,” *Journal of Neurosurgery*, 109(4), pp. 615–624. doi: 10.3171/JNS/2008/109/10/0615.

Groppa, S. *et al.* (2012) “A practical guide to diagnostic transcranial magnetic stimulation: Report of an IFCN committee,” *Clinical Neurophysiology*. International Federation of Clinical Neurophysiology, 123(5), pp. 858–882. doi: 10.1016/j.clinph.2012.01.010.

Hallett, M. (2000) “Transcranial magnetic stimulation and the human brain,” *Nature*. Nature Publishing Group, 406(6792), pp. 147–150. doi: 10.1038/35018000.

Hallett, M. (2007) “Transcranial Magnetic Stimulation: A Primer,” *Neuron*. Elsevier, 55(2), pp. 187–199. doi: 10.1016/j.neuron.2007.06.026.

Hayashi, Y. *et al.* (2014) “Functional reorganization in the patient with progressing glioma of the pure primary motor cortex: A case report with special reference to the topographic central sulcus defined by somatosensory-evoked potential,” *World Neurosurgery*. Elsevier Inc, 82(3), pp. 536.E1-536.E4. doi: 10.1016/j.wneu.2013.01.084.

Hayhurst, C. (2017) “Contemporary management of low-grade glioma: A paradigm shift in neuro-oncology,” *Practical Neurology*, 17(3), pp. 183–190. doi: 10.1136/practneurol-2017-001604.

Heiss, W.-D. *et al.* (2003) “Disturbance and recovery of language function: correlates in PET activation studies,” *NeuroImage*, 20, pp. S42–S49. doi: https://doi.org/10.1016/j.neuroimage.2003.09.005.

Hervey-Jumper, S. L. and Berger, M. S. (2016) “Maximizing safe resection of low- and high-grade glioma,” *Journal of Neuro-Oncology*, 130(2), pp. 269–282. doi: 10.1007/s11060-016-2110-4.

Hess, B. Y. C. W., Mills, K. R. and Murray, N. M. F. (1987) “Responses in small hand muscles from magnetic stimulation of the human brain,” *Journal of Physiology*, pp. 397–419.

Hollon, T. *et al.* (2015) “Advances in the Surgical Management of Low-Grade Glioma,” *Seminars in Radiation Oncology*, 25(3), pp. 181–188. doi: 10.1016/j.semradonc.2015.02.007.

Horvath, J. C. *et al.* (2011) “Transcranial magnetic stimulation: A historical evaluation and future prognosis of therapeutically relevant ethical concerns,” *Journal of Medical Ethics*, 37(3), pp. 137–143. doi: 10.1136/jme.2010.039966.

Iimori, T. *et al.* (2019) “Effectiveness of the prefrontal repetitive transcranial magnetic stimulation on cognitive profiles in depression, schizophrenia, and Alzheimer’s disease: A systematic review,” *Progress in Neuro-Psychopharmacology and Biological Psychiatry*, 88(June 2018), pp. 31–40. doi: 10.1016/j.pnpbp.2018.06.014.

Ille, S. *et al.* (2018) “Mapping of Arithmetic Processing by Navigated Repetitive Transcranial Magnetic Stimulation in Patients with Parietal Brain Tumors and Correlation with Postoperative Outcome,” *World Neurosurgery*. Elsevier Inc., 114, pp. e1016–e1030. doi: 10.1016/j.wneu.2018.03.136.

Ius, T. *et al.* (2011) “Evidence for potentials and limitations of brain plasticity using an atlas of functional resectability of WHO grade II gliomas: towards a ‘minimal common brain’.,” *NeuroImage*. Elsevier Inc., 56(3), pp. 992–1000. doi: 10.1016/j.neuroimage.2011.03.022.

Jacobs, K. and Donoghue, J. (1991) “Reshaping the cortical motor map by unmasking latent intracortical connections,” *Science*, 251(4996), pp. 944–947. doi: 10.1126/science.2000496.

Jacobs, K. M. (2011) “Brodmann’s Areas of the Cortex,” in Kreutzer, J. S., DeLuca, J., and Caplan, B. (eds.) *Encyclopedia of Clinical Neuropsychology*. New York, NY: Springer, pp. 459–459. doi: 10.1007/978-0-387-79948-3_301.

Janicak, P. G. *et al.* (2013) “Transcranial magnetic stimulation (TMS) for major depression: A multisite, naturalistic, observational study of quality of life outcome measures in clinical practice,” *CNS Spectrums*, 18(6), pp. 322–332. doi: 10.1017/S1092852913000357.

Jung, J. *et al.* (2019) “First United Kingdom Experience of Navigated Transcranial Magnetic Stimulation in Preoperative Mapping of Brain Tumors,” *World Neurosurgery*, 122, pp. e1578–e1587. doi: 10.1016/j.wneu.2018.11.114.

Kew, J. J. *et al.* (1994) “Reorganization of cortical blood flow and transcranial magnetic stimulation maps in human subjects after upper limb amputation,” *Journal of Neurophysiology*, 72(5), pp. 2517–2524. doi: 10.1152/jn.1994.72.5.2517.

Kim, Y.-H. H. *et al.* (2006) “Repetitive transcranial magnetic stimulation-induced corticomotor excitability and associated motor skill acquisition in chronic stroke,” *Stroke*, 37(6), pp. 1471–1476. doi: 10.1161/01.STR.0000221233.55497.51.

Klomjai, W., Katz, R. and Lackmy-Vallée, A. (2015) “Basic principles of transcranial magnetic stimulation (TMS) and repetitive TMS (rTMS),” *Annals of Physical and Rehabilitation Medicine*, 58(4), pp. 208–213. doi: 10.1016/j.rehab.2015.05.005.

Koenraadt, K. L. M. *et al.* (2011) “TMS: a navigator for NIRS of the primary motor cortex?,” *Journal of neuroscience methods*. Elsevier B.V., 201(1), pp. 142–8. doi: 10.1016/j.jneumeth.2011.07.024.

Krainik, A. *et al.* (2004) “Role of the healthy hemisphere in recovery after resection of the supplementary motor area,” *Neurology*. Lippincott Williams & Wilkins, 62(8), pp. 1323–1332. doi: 10.1212/01.WNL.0000120547.83482.B1.

Krieg, S. M. *et al.* (2012) “Utility of presurgical navigated transcranial magnetic brain stimulation for the resection of tumors in eloquent motor areas,” *Journal of Neurosurgery*, 116(5), pp. 994–1001.

Krieg, S. M. *et al.* (2013) “Presurgical navigated transcranial magnetic brain stimulation for recurrent gliomas in motor eloquent areas,” *Clinical Neurophysiology*, 124(3), pp. 522–527. doi: 10.1016/j.clinph.2012.08.011.

Krieg, S. M., Sabih, J., *et al.* (2014) “Preoperative motor mapping by navigated transcranial magnetic brain stimulation improves outcome for motor eloquent lesions,” *Neuro-Oncology*, 16(9), pp. 1274–1282. doi: 10.1093/neuonc/nou007.

Krieg, S. M., Sollmann, N., *et al.* (2014) “Repeated mapping of cortical language sites by preoperative navigated transcranial magnetic stimulation compared to repeated intraoperative DCS mapping in awake craniotomy,” *BMC Neuroscience*. BMC Neuroscience, 15(1), p. 20. doi: 10.1186/1471-2202-15-20.

Lavrador, J. P. *et al.* (2020) “Pre- and Intraoperative Mapping for Tumors in the Primary Motor Cortex: Decision-Making Process in Surgical Resection,” *Journal of Neurological Surgery Part A: Central European Neurosurgery*, (May). doi: 10.1055/s-0040-1709729.

Liepert, J. *et al.* (1998) “Motor cortex plasticity during constraint, induced movement therapy in stroke patients,” *Neuroscience Letters*, 250(1), pp. 5–8. doi: 10.1016/S0304-3940(98)00386-3.

Lioumis, P. *et al.* (2012) “A novel approach for documenting naming errors induced by navigated transcranial magnetic stimulation,” *Journal of Neuroscience Methods*. Elsevier B.V., 204(2), pp. 349–354. doi: 10.1016/j.jneumeth.2011.11.003.

Louis, D. N. *et al.* (2016) “The 2016 World Health Organization Classification of Tumors of the Central Nervous System: a summary,” *Acta Neuropathologica*, 131(6), pp. 803–820. doi: 10.1007/s00401-016-1545-1.

Mano, Y. *et al.* (1995) “Central motor reorganization after anastomosis of the musculocutaneous and intercostal nerves following cervical root avulsion,” *Annals of Neurology*, 38(1), pp. 15–20. doi: 10.1002/ana.410380106.

Marko, N. F. *et al.* (2014) “Extent of resection of glioblastoma revisited: Personalized survival modeling facilitates more accurate survival prediction and supports a maximum-safe-resection approach to surgery,” *Journal of Clinical Oncology*, 32(8), pp. 774–782. doi: 10.1200/JCO.2013.51.8886.

Martino, J. *et al.* (2009) “Re-operation is a safe and effective therapeutic strategy in recurrent WHO grade II gliomas within eloquent areas,” *Acta Neurochirurgica*, 151(5), pp. 427–436. doi: 10.1007/s00701-009-0232-6.

Massé-Alarie, H. *et al.* (2017) “‘Discrete peaks’ of excitability and map overlap reveal task-specific organization of primary motor cortex for control of human forearm muscles,” *Human Brain Mapping*, 38(12), pp. 6118–6132. doi: 10.1002/hbm.23816.

McGregor, K. M. *et al.* (2012) “Motor map reliability and aging: a TMS/fMRI study,” *Experimental Brain Research*, 219(1), pp. 97–106. doi: 10.1007/s00221-012-3070-3.

Merton, P. A. and Morton, H. B. (1980) “Stimulation of the cerebral cortex in the intact human subject,” *Nature*, 285, p. 227. doi: 10.1038/285227a0.

Mills, K. R., Boniface, S. J. and Schubert, M. (1992) “Magnetic brain stimulation with a double coil: the importance of coil orientation,” *Electroencephalography and Clinical Neurophysiology/ Evoked Potentials*, 85(1), pp. 17–21. doi: 10.1016/0168-5597(92)90096-T.

Moser, T. *et al.* (2017) “Resection of Navigated Transcranial Magnetic Stimulation-Positive Prerolandic Motor Areas Causes Permanent Impairment of Motor Function,” *Neurosurgery*, 81(1), pp. 99–109. doi: 10.1093/neuros/nyw169.

Naeser, M. A. *et al.* (2011) “TMS suppression of right pars triangularis, but not pars opercularis, improves naming in aphasia,” *Brain and Language*, 119(3), pp. 206–213. doi: 10.1016/j.bandl.2011.07.005.

Ngomo, S. *et al.* (2012) “Comparison of transcranial magnetic stimulation measures obtained at rest and under active conditions and their reliability.,” *Journal of neuroscience methods*, 205(1), pp. 65–71. doi: 10.1016/j.jneumeth.2011.12.012.

Nii, Y. *et al.* (1996) “Does the central sulcus divide motor and sensory functions? Cortical mapping of human hand areas as revealed by electrical stimulation through subdural grid electrodes,” *Neurology*, 46(2), pp. 360–367. doi: 10.1212/WNL.46.2.360.

Ojemann, J. G., Miller, J. W. and Silbergeld, D. L. (1996) “Preserved function in brain invaded by tumor,” *Neurosurgery*, 39(2), pp. 253–259. doi: 10.1097/00006123-199608000-00003.

Opitz, A. *et al.* (2013) “Physiological observations validate finite element models for estimating subject-specific electric field distributions induced by transcranial magnetic stimulation of the human motor cortex.,” *NeuroImage*. The Authors, 81, pp. 253–64. doi: 10.1016/j.neuroimage.2013.04.067.

Opitz, A. *et al.* (2014) “Validating computationally predicted TMS stimulation areas using direct electrical stimulation in patients with brain tumors near precentral regions.,” *NeuroImage. Clinical*, 4, pp. 500–7. doi: 10.1016/j.nicl.2014.03.004.

Ostrom, Q. T. *et al.* (2017) “Epidemiology of Intracranial Gliomas,” *Progress in Neurological Surgery*, 30, pp. 1–11. doi: 10.1159/000464374.

Ottenhausen, M. *et al.* (2015) “Functional preoperative and intraoperative mapping and monitoring: increasing safety and efficacy in glioma surgery,” *Neurosurgical focus*, 38(January), pp. 1–13. doi: 10.3171/2014.10.FOCUS14611.Disclosure.

Paillard, J. (1976) “Reflexions Sur L’Usage Du Concept De Plasticite En Neurobiologie,” *Journal de Psychologie Normale et Pathologique*, 73(1), pp. 33–47.

Pascual-Leone, A. *et al.* (1994) “Akinesia in Parkinson’s disease. II. Effects of subthreshold repetitive transcranial motor cortex stimulation,” *Neurology*, 44(5), pp. 892–898. doi: 10.1212/wnl.44.5.892.

Pascual-Leone, A., Bartres-Faz, D. and Keenan, J. P. (1999) “Transcranial magnetic stimulation: studying the brain-behaviour reltionship by induction of ‘virtual lesions,’” *Philos. Trans. Royal Soc. B*, 354(1387), pp. 1229–1238. doi: 10.1098/rstb.1999.0476.

Pascual-Leone, A., Gates, J. R. and Dhuna, A. (1991) “Induction of speech arrest and counting errors with rapid-rate transcranial magnetic stimulation,” *Neurology*, 41(5), pp. 697–702. doi: 10.1212/WNL.41.5.697.

Paulus, W., Peterchev, A. V and Ridding, M. (2013) “Transcranial electric and magnetic stimulation: technique and paradigms.,” in Lozano, A. M. and Hallett, M. (eds.) *Handbook of clinical neurology*. Elsevier B.V., pp. 329–342. doi: 10.1016/B978-0-444-53497-2.00027-9.

Penfield, W. and Boldrey, E. (1937) “Somatic Motor and Sensory Representation in,” *Brain: A Journal of Neurology*, 60, pp. 389–443. doi: 10.1093/brain/60.4.389.

Perera, T. *et al.* (2016) “The Clinical TMS Society Consensus Review and Treatment Recommendations for TMS Therapy for Major Depressive Disorder,” *Brain Stimulation*, 9(3), pp. 336–346. doi: 10.1016/j.brs.2016.03.010.

Picht, T. *et al.* (2013) “A comparison of language mapping by preoperative navigated transcranial magnetic stimulation and direct cortical stimulation during awake surgery,” *Neurosurgery*, 72(5), pp. 808–819. doi: 10.1227/NEU.0b013e3182889e01.

Puderbaugh, M. and Emmady, P. (2021) *Neuroplasticity.*, *StatPearls*. Available at: https://www-ncbi-nlm-nih-gov.eaccess.ub.tum.de/books/NBK557811/.

Ravazzani, P. *et al.* (1996) “Magnetic Stimulation of the Nervous System: Induced Electric Field in Unbounded, Semi-infinite, Spherical, and Cylindrical Media,” *Annals of Biomedical Engineering*, 24(5), pp. 606–616.

Reifenberger, G. *et al.* (2016) “Advances in the molecular genetics of gliomas — implications for classification and therapy,” *Nature Reviews Clinical Oncology*, 14(7), pp. 434–452. doi: 10.1038/nrclinonc.2016.204.

Reni, M. *et al.* (2017) “Central nervous system gliomas,” *Critical Reviews in Oncology/Hematology*. Elsevier Ireland Ltd, 113, pp. 213–234. doi: 10.1016/j.critrevonc.2017.03.021.

Rijntjes, M. *et al.* (1997) “Cortical reorganization in patients with facial palsy,” *Annals of Neurology*, 41(5), pp. 621–630. doi: 10.1002/ana.410410511.

Rijntjes, M. and Weiller, C. (2002) “Recovery of motor and language abilities after stroke: The contribution of functional imaging,” *Progress in Neurobiology*, 66(2), pp. 109–122. doi: 10.1016/S0301-0082(01)00027-2.

Rösler, J. *et al.* (2014) “Language mapping in healthy volunteers and brain tumor patients with a novel navigated TMS system: evidence of tumor-induced plasticity.,” *Clinical neurophysiology : official journal of the International Federation of Clinical Neurophysiology*, 125(3), pp. 526–36. doi: 10.1016/j.clinph.2013.08.015.

Rossini, P. M. *et al.* (2015) “Non-invasive electrical and magnetic stimulation of the brain, spinal cord, roots and peripheral nerves: basic principles and procedures for routine clinical and research application. An updated report from an I.F.C.N. Committee,” *Clinical Neurophysiology*, 126(6), pp. 1071–1107. doi: 10.1016/j.clinph.2015.02.001.

Rudà, R. *et al.* (2012) “Seizures in low-grade gliomas: natural history, pathogenesis, and outcome after treatments.,” *Neuro-oncology*, 14 Suppl 4(Suppl 4), pp. iv55-64. doi: 10.1093/neuonc/nos199.

Ruohonen, J. and Ilmoniemi, R. J. (1999) “Modeling of the stimulating field generation in TMS.,” *Electroencephalography and clinical neurophysiology. Supplement*, pp. 30–40.

Ruohonen, J. and Karhu, J. (2010) “Navigated transcranial magnetic stimulation.,” *Neurophysiologie clinique*. Elsevier Masson SAS, 40(1), pp. 7–17. doi: 10.1016/j.neucli.2010.01.006.

Sakai, K. *et al.* (1997) “Preferential activation of different I waves by transcranial magnetic stimulation with a figure-of-eight-shaped coil,” *Experimental Brain Research*, 113(1), pp. 24–32. doi: 10.1007/BF02454139.

Sanai, N. and Berger, M. S. (2010) “Intraoperative stimulation techniques for functional pathway preservation and glioma resection,” *Neurosurgical Focus*, 28(2), pp. 1–9. doi: 10.3171/2009.12.FOCUS09266.

Sanai, N. and Berger, M. S. (2011) “Extent of resection influences outcomes for patients with gliomas,” *Revue Neurologique*, 167(10), pp. 648–654. doi: 10.1016/j.neurol.2011.07.004.

Sandrini, M. and Cohen, L. G. (2013) “Noninvasive brain stimulation in neurorehabilitation.,” in Lozano, A. M. and Hallett, M. (eds.) *Handbook of clinical neurology*. 1st ed. Elsevier, pp. 499–524. doi: 10.1016/B978-0-444-53497-2.00040-1.

Sanes, J. N. J. and Donoghue, J. P. J. (2000) “Plasticity and primary motor cortex,” *Annu Rev Neurosci*, 23, p. 393-415. doi: 10.1146/annurev.neuro.23.1.393.

Sanes, J. N., Suner, S. and Donoghue, J. P. (1990) “Dynamic organization of primary motor cortex output to target muscles in adult rats I. Long-term patterns of reorganization following motor or mixed peripheral nerve lesions,” *Experimental Brain Research*, 79(3), pp. 479–491. doi: 10.1007/BF00229318.

Schieber, M. H. (2001) “Constraints on somatotopic organization in the primary motor cortex,” *Journal of Neurophysiology*, 86(5), pp. 2125–2143. doi: 10.1152/jn.2001.86.5.2125.

Schiffbauer, H. *et al.* (2001) “Functional activity within brain tumors: A magnetic source imaging study,” *Neurosurgery*, 49(6), pp. 1313–1321. doi: 10.1097/00006123-200112000-00005.

Schucht, P. *et al.* (2014) “5-ALA complete resections go beyond MR contrast enhancement: shift corrected volumetric analysis of the extent of resection in surgery for glioblastoma,” *Acta Neurochirurgica*, 156(2), pp. 305–312. doi: 10.1007/s00701-013-1906-7.

Schucht, P. *et al.* (2015) “Extending resection and preserving function: Modern concepts of glioma surgery,” *Swiss Medical Weekly*, 145(February), pp. 1–11. doi: 10.4414/smw.2015.14082.

Seitz, R. J. and Freund, H. J. (1997) “Plasticity of the human motor cortex.,” *Advances in neurology*. Berlin, Heidelberg: Springer Berlin Heidelberg, pp. 321–333. doi: 10.1007/978-3-642-78367-8_6.

Sessle, B. and Wiesendanger, M. (1982) “Structural and functional definition of the motor cortex in the monkey (macaca fascicularis),” *Journal of Physiology*, 323(1), pp. 245–265. doi: 10.1113/jphysiol.1982.sp014071.

Siebner, H. R. *et al.* (1999) “Repetitive transcranial magnetic stimulation has a beneficial effect on bradykinesia in Parkinson’s disease,” *NeuroReport*, 10(3), pp. 589–594. doi: 10.1097/00001756-199902250-00027.

Sollmann, N. *et al.* (2013) “Inter- and intraobserver variability in motor mapping of the hotspot for the abductor policis brevis muscle.,” *BMC neuroscience*, 14, p. 94. doi: 10.1186/1471-2202-14-94.

Sollmann, N., Wildschuetz, N., *et al.* (2018) “Associations between clinical outcome and navigated transcranial magnetic stimulation characteristics in patients with motor-eloquent brain lesions: A combined navigated transcranial magnetic stimulation-diffusion tensor imaging fiber tracking approach,” *Journal of Neurosurgery*, 128(3), pp. 800–810. doi: 10.3171/2016.11.JNS162322.

Sollmann, N., Laub, T., *et al.* (2018) “Predicting brain tumor regrowth in relation to motor areas by functional brain mapping,” *Neuro-Oncology Practice*, 5(2), pp. 82–95. doi: 10.1093/nop/npx021.

Suchorska, B. *et al.* (2016) “Complete resection of contrast-enhancing tumor volume is associated with improved survival in recurrent glioblastoma - Results from the DIRECTOR trial,” *Neuro-Oncology*, 18(4), pp. 549–556. doi: 10.1093/neuonc/nov326.

Takahashi, S. *et al.* (2012) “Plastic relocation of motor cortex in a patient with LGG (low grade glioma) confirmed by NBS (navigated brain stimulation),” *Acta Neurochirurgica*. Springer-Verlag, 154(11), pp. 2003–2008. doi: 10.1007/s00701-012-1492-0.

Tamura, M. *et al.* (2015) “Strategy of Surgical Resection for Glioma Based on Intraoperative Functional Mapping and Monitoring,” *Neurologia medico-chirurgica*, 55(5), pp. 383–398. doi: 10.2176/nmc.ra.2014-0415.

Tarapore, P. E. *et al.* (2016) “Safety and tolerability of navigated TMS for preoperative mapping in neurosurgical patients.,” *Clinical Neurophysiology*, 127(3), pp. 1895–1900. doi: 10.1016/j.clinph.2015.11.042.

Teitti, S. *et al.* (2008) “Non-primary motor areas in the human frontal lobe are connected directly to hand muscles,” *NeuroImage*, 40(3), pp. 1243–1250. doi: 10.1016/j.neuroimage.2007.12.065.

Thickbroom, G. W., Sammut, R. and Mastaglia, F. L. (1998) “Magnetic stimulation mapping of motor cortex: factors contributing to map area.,” *Electroencephalography and clinical neurophysiology*, 109(2), pp. 79–84.

Thielscher, A., Opitz, A. and Windhoff, M. (2011) “Impact of the gyral geometry on the electric field induced by transcranial magnetic stimulation.,” *NeuroImage*. Elsevier Inc., 54(1), pp. 234–243. doi: 10.1016/j.neuroimage.2010.07.061.

Ungerleider, L. G., Doyon, J. and Karni, A. (2002) “Imaging brain plasticity during motor skill learning.,” *Neurobiology of learning and memory*. United States, 78(3), pp. 553–564. doi: 10.1006/nlme.2002.4091.

Weiller, C. (1998) “Imaging recovery from stroke,” *Experimental Brain Research*, 123(1), pp. 13–17. doi: 10.1007/s002210050539.

Weiss, C. *et al.* (2013) “Mapping the hand, foot and face representations in the primary motor cortex - retest reliability of neuronavigated TMS versus functional MRI.,” *NeuroImage*. Elsevier Inc., 66, pp. 531–542. doi: 10.1016/j.neuroimage.2012.10.046.

Will, B. *et al.* (2008) “The concept of brain plasticity – Paillard’s systemic analysis and emphasis on structure and function. (followed by the translation of a seminal paper by Paillard on plasticity),” *Behavioural Brain Research*, 192(1), pp. 2–7. doi: 10.1016/j.bbr.2007.11.008.

Wolf, S. L. *et al.* (2004) “Intra-subject reliability of parameters contributing to maps generated by transcranial magnetic stimulation in able-bodied adults.,” *Clinical neurophysiology : official journal of the International Federation of Clinical Neurophysiology*, 115(8), pp. 1740–7. doi: 10.1016/j.clinph.2004.02.027.

Yordanova, Y. N. and Duffau, H. (2017) “Supratotal resection of diffuse gliomas – an overview of its multifaceted implications,” *Neurochirurgie*, 63(3), pp. 243–249. doi: 10.1016/j.neuchi.2016.09.006.

Yousry, T. A. *et al.* (1997) “Localization of the motor hand area to a knob on the precentral gyrus. A new landmark.,” *Brain*, 120(1), pp. 141–157. doi: 10.1093/brain/120.1.141.

11. PUBLICATIONS

Original papers

Conway, N., Wildschuetz, N., Moser, T., Bulubas, L., Sollmann, N., Tanigawa, N., Meyer, B., Krieg, S.M. (2017) “Cortical plasticity of motor-eloquent areas measured by navigated transcranial magnetic stimulation in patients with glioma,” *Journal of Neurosurgery*, 127(5), pp. 981–991. doi: 10.3171/2016.9.JNS161595.

Ille, S., Drummer, K., Giglhuber, K., Conway, N., Maurer, S., Meyer, B., Krieg, S.M. (2018) “Mapping of Arithmetic Processing by Navigated Repetitive Transcranial Magnetic Stimulation in Patients with Parietal Brain Tumors and Correlation with Postoperative Outcome,” *World Neurosurgery*. Elsevier Inc., 114, pp. e1016–e1030. doi: 10.1016/j.wneu.2018.03.136.

Moser, T., Bulubas, L., Sabih, J., Conway, N., Wildschuetz, N., Sollmann, N., Meyer, B., Ringel, F., Krieg, S.M. (2017) “Resection of Navigated Transcranial Magnetic Stimulation-Positive Prerolandic Motor Areas Causes Permanent Impairment of Motor Function,” *Neurosurgery*, 81(1), pp. 99–109. doi: 10.1093/neuros/nyw169.

Sollmann, N., Wildschuetz, N., Kelm, A., Conway, N., Moser, T., Bulubas, L., Kirschke, J.S., Meyer, B. Krieg, S.M. (2018) “Associations between clinical outcome and navigated transcranial magnetic stimulation characteristics in patients with motor-eloquent brain lesions: A combined navigated transcranial magnetic stimulation-diffusion tensor imaging fiber tracking approach,” *Journal of Neurosurgery*, 128(3), pp. 800–810. doi: 10.3171/2016.11.JNS162322.

Oral presentations

Conway, N., Wildschuetz, N., Moser, T., Bulubas, L., Tanigawa, N., Sabih, J., Sollmann, N., Meyer, B., Krieg, S.M. “Cortical plasticity of motor-eloquent areas measured using navigated transcranial magnetic stimulation in glioma patients”

Meeting: Sektionstagung Neurophysiologie der Deutschen Gesellschaft für Neurochirurgie, München, 23.-24.10.2015

Posters

Conway, N., Wildschuetz, N., Moser, T., Bulubas, L., Tanigawa, Sabih, J., N., Meyer, B., Krieg, S.M. (2015) “Cortical plasticity of motor-eloquent areas measured by navigated transcranial stimulation in glioma patients”

Meeting: 6th International Symposium on NBS in Neurosurgery, Berlin, 10.-11.10.2015

Conway, N., Wildschuetz, N., Moser, T., Bulubas, L., Sollmann, N., Ille, S., Tanigawa, N., Meyer, B., Krieg, S.M. “Cortical plasticity of motor-eloquent areas measured by navigated transcranial stimulation in glioma patients”

Meeting: 84th AANS Annual Scientific Meeting, Chicago, 30.04.-04.05.2016

Conway, N., Wildschuetz, N., Moser, T., Bulubas, L., Sollmann, N., Tanigawa, N., Meyer, B., Krieg, S.M. “Cortical plasticity of motor-eloquent areas measured by navigated transcranial stimulation in glioma patients”

Meeting: 16th European Congress of Neurosurgery, Athens, 4.-8.09.2016

Conway, N., Tanigawa, N., Meyer, B., Krieg, S.M. “Cortical plasticity of motor-eloquent areas measured by navigated transcranial stimulation in glioma patients”

Meeting: Congress of Neurological Surgeons Annual Meeting, San Diego, 24.-28.09.2016

12. ACKNOWLEDGEMENTS

First of all, I owe great thanks to apl. Prof. Dr. Sandro M. Krieg. His dedication, drive and perseverance are unrivalled, and I am grateful to him for sharing his knowledge and advice whenever called upon. I am grateful that he introduced me to scientific work, and reliably pushed me, with just the right amount of insistence, to finish what we started.

I would like to thank the members and partners of our research group for their help, team spirit and drive. An incomplete, alphabetical list includes Lucia Bulubas, Vicki Butenschön, Katrin Giglhuber, Moritz Goblirsch-Kolb, Theresa Hauck, Sebastian Ille, Anna Kelm, Stephanie Maurer, Tobias Moser, Chiara Negwer, Axel Schröder Nico Sollmann, Noriko Tanigawa, Noémie Wildschuetz and Regina Wittig.

I thank Univ.-Prof. Dr. Bernhard Meyer as Head of the Department of Neurosurgery at University Hospital rechts der Isar, and his former Vice Chairman Univ.-Prof. Dr. Florian Ringel, as well as PD Dr. Christian Sorg, for agreeing to make this thesis possible.

Particular thanks go to my parents, brother, family and friends for their love and support. I am sure they will be relieved to know this particular chapter is finally closed. Most of all I thank Sarah, for putting up with me, and patiently putting everything into perspective.